UC San Diego
UC San Diego Previously Published Works

Title

FOXO1 constrains activation and regulates senescence in CD8 T cells

Permalink

Journal

Cell Reports, 34(4)

ISSN

2639-1856

Authors

Delpoux, Arnaud
Marcel, Nimi
Hess Michelini, Rodrigo
et al.

Publication Date

2021

DOI

10.1016/j.celrep.2020.108674

Peer reviewed

FOXO1 constrains activation and regulates senescence in CD8 T cells

Arnaud Delpoux[1,2], Nimi Marcel[1,2], Rodrigo Hess Michelini[1,2], Carol D. Katayama[1,2], Karmel A. Allison[2], Christopher K. Glass[2], Sergio M. Quiñones-Parra[1], Cornelis Murre[1], Liyen Loh[3], Katherine Kedzierska[3], Martha Lappas[4], Stephen M. Hedrick[1,2]*‡, Andrew L. Doedens[1,2]*

[1]Division of Biological Sciences, Molecular Biology Section

[2]Department of Cellular and Molecular Medicine
 University of California, San Diego
 9500 Gilman Drive
 La Jolla, CA 92093-0377
 USA

[3]Department of Microbiology and Immunology, University of Melbourne, Peter Doherty Institute for Infection
 and Immunity, Parkville, Victoria, Australia

[4]Obstetrics, Nutrition and Endocrinology Group, Department of Obstetrics & Gynaecology, University of
 Melbourne, Mercy Hospital for Women

*Corresponding authors: shedrick@ucsd.edu; adoedens@gmail.com

‡Lead contact

Summary

Naïve and memory T cells are maintained in a quiescent state, yet capable of rapid response and differentiation to antigen challenge via molecular mechanisms that are not fully understood. In naive cells, deletion of *Foxo1* following thymic development resulted in increased expression of multiple AP-1 family members, rendering T cells less able to respond to antigenic challenge. Similarly, in the absence of FOXO1, post-infection memory T cells exhibited characteristics of extended activation and senescence. Age-based analysis of human peripheral T cells revealed that levels of FOXO1 and its downstream target, TCF7, were inversely related to host age, whereas the opposite was found for AP-1 factors. These characteristics of aging also correlated with the with the formation of T cells manifesting features of cellular senescence. Our work illustrates a role for FOXO1 in the active maintenance of stem-like properties in T cells at the time-scales of acute infection and organismal life-span.

Introduction

Relative to stem cells, newly formed T cells are highly differentiated, yet maintain qualities of self-renewal, an ability to repeatedly enter and exit the cell cycle, and plasticity with regard to further differentiation. These properties contribute to a host's continuing ability to attain adaptive immunity to novel pathogens, while at the same time maintain a large repertoire of T cells that can serially or continually respond to persistent infections. With age, however, naïve and memory T cells shift to a more differentiated state, and take on a senescent phenotype that restricts their ability to respond to an antigenic stimulus and proliferate without loss of viability (Goronzy and Weyand, 2017; Gustafson et al., 2018). The molecular mechanisms governing T cell self-renewal, differentiation capacity, and the changes observed in aged individuals are not fully understood.

The FOXO family of transcription factors display pro-longevity characteristics first discovered in genetic screens of *C. elegans* (Kenyon et al., 1993; Gottlieb and Ruvkun, 1994). These features extend across phyla as FOXO1 and FOXO3 polymorphisms are linked to exceptional longevity in multiple human populations throughout the world (Lunetta et al., 2007; Li et al., 2009; Kenyon, 2010). The basis for this is likely to be complex, but one relevant aspect may be a role for FOXO1 in the active suppression of cellular differentiation. This has been shown for pluripotent human and mouse embryonic stem cells (Zhang et al., 2011) as well as organ-specific stem cells with more limited differentiation potential (Liang and Ghaffari, 2018; McLaughlin and Broihier, 2018). For lymphocytes, FOXO1 is essential for the induction of memory T cells capable of self-renewal and re-expansion in response to antigenic stimulation (Rao et al., 2012; Hess Michelini et al., 2013; Kim et al., 2013; Tejera et al., 2013), as it promotes the partitioning of memory and effector subsets within days of a viral infection (Delpoux et al., 2017). It is furthermore necessary for the maintenance of a memory state in T cells poised to respond to antigen (Delpoux et al., 2018; Utzschneider et al., 2018). FOXO1 appears to be regulated, in part, as a target of miRNA regulation that correlates with altered naïve T cell homeostasis during human aging (Gustafson et al., 2018).

Here, we show that FOXO1 actively maintains T cell quiescence and proliferative potential such that, in its absence, naïve T cells up-regulate a subset of post-activation effector transcripts such as *Ifng*. Initially, this correlated with the activation of the AP-1 family of transcription factors, heterodimeric complexes that bind to palindromic 12-*O*-tetradecanoylphorbol-13-acetate (TPA) response elements (TREs; 5′-TGA (C/G)TCA-3′) (Turner and Tjian, 1989; Foletta et al., 1998; Shaulian and Karin, 2002a); however, upon antigen-induced T cell activation, the regulation of AP-1 factors was found to be mechanistically transferred to the gene encoding BACH2, itself a direct target of FOXO1 (Roychoudhuri et al., 2016; Tamahara et al., 2017). These findings led us to an examination of human T cells partitioned by phenotype or age that followed a progression toward senescence, and this progression was closely correlated with the extent of FOXO1 expression and a direct target, *Tcf7*. Altogether, we conclude that FOXO1 functions in T cells to actively prevent terminal differentiation and senescence, and it is essential to maintain the ability of T cells to effectively respond to primary or subsequent stimulation. We propose AP-1 inhibition as one of the intrinsic mechanisms by which FOXO1 attenuates effector program and maintains T cell proliferation and

differentiation capacities among antigen-specific T cells.

Results

FOXO1 maintains quiescence in naïve T cells

To determine how gene expression changes in naïve cells with long-term *Foxo1* deletion, T cells from *Foxo1*f/f dLck-Cre (*Foxo1*-KO) mice were compared with *Foxo1*f/f mice by RNA-seq (Figure 1A). In dLck-Cre transgenic mice, CRE-recombinase (CRE) was shown to be expressed during thymus development subsequent to positive selection when CD3 is expressed at high levels and the thymocytes express either CD4 or CD8. In T cells found in the secondary lymphoid organs, CRE was shown to be expressed in greater than 90% of mature CD8$^+$ T cells, but less than 75% of CD4$^+$ T cells (Zhang et al., 2005). Thus, in *Foxo1*-KO mice, *Foxo1* is deleted subsequent to thymic selection, and yet there are sufficient CD4$^+$ FOXO1$^+$ FOXP3$^+$ T cells to prevent spontaneous autoimmunity. The mice did not manifest any of the autoimmune characteristics of *Foxo1*f/f *Cd4*-Cre mice (Kerdiles et al., 2010). Genes that were more highly expressed in the WT vs. *Foxo1*-KO cells in addition to *Foxo1* included *Il7r* (Kerdiles et al., 2009), *Klrd1* (CD94-known to be induced on activated CD8$^+$ T cells), and *Scarna2*, a LncRNA of unknown function (Zhang et al., 2019). However, the major effect observed in naïve *Foxo1*-KO T cells was gene expression usually associated with T cell activation. Induced genes included *Nr4a1* (Nur77), *Egr1*, *Ccl5* (Rantes), and *Ifng*, but in addition, a number of genes encoding subunits of the complex AP-1 family including: *FosB*, *Fos*, *Jun*, *JunB*, *JunD*, and *Atf3* (Figure 1A).

These data imply that FOXO1 is required to maintain a quiescent state in naïve T cells. To test for the regulation of FOXO1 before and during a viral infection, we analyzed the expression of total FOXO1 and a phosphorylated form of FOXO1 (S256 in human, S253 in mice) characteristic of exclusion from the nucleus (Calnan and Brunet, 2008). P14 T cells from naïve mice, or mice that were infected with LCMV-Armstrong (LCMV-ARM) for either 7 or 12 days were isolated and activated for various times in culture. The lysates were then analyzed for FOXO1, pFOXO1, and β-tubulin as a control (Figure S1). Naïve T cells prior to activation strongly expressed FOXO1 in an unphosphorylated form, and with activation in culture, phosphorylation plateaued at approximately 30 minutes. As pFOXO1 increased, the total amount of FOXO1 decreased consistent with the well-established regulation of FOXO1 based on phosphorylation by AKT or SGK1 (Brunet et al., 2001; Guertin et al., 2006) resulting in nuclear export and degradation by 14-3-3 (Van Der Heide et al., 2004). LCMV-specific T cells isolated from mice infected for 7 days showed a similar, albeit exaggerated FOXO1 phosphorylation following activation in culture. From many previous studies (Kaech and Wherry, 2007), this population largely consists of cytotoxic effector cells. T cells from mice infected 12 days earlier displayed low amounts of FOXO1 that once again diminished with phosphorylation (Figure S1).

To verify that the differences in AP-1 gene expression were also reflected in protein expression, we analyzed the expression of FOS, JUNB, and FOSB in CD44^{low} (naïve) and CD44^{high} (previously activated) T cells. For comparison, we analyzed mice in which FOXO1 is constitutively nuclear via the transgenic expression of a

Foxo1-triple alanine phosphorylation mutant (*Foxo1*-AAA) (Burgering and Kops, 2002; Ouyang et al., 2012; Stone et al., 2015). Consistent with FOXO1 repression of AP-1 factor expression in naïve T cells, we found FOS, JUNB, and FOSB to be relatively high in T cells from *Foxo1*-KO, intermediate in T cells from WT, and diminished in T cells from *Foxo1*-AAA mice (Figure 1B).

To explore direct FOXO1 regulation of AP-1 family genes, we performed ChIP-seq on chromatin bound by FOXO1 in naive P14 T cells from unimmunized mice, or P14 T cells harvested from host mice 12 days after infection with LCMV-ARM; also, we analyzed open chromatin in naïve P14 and P14 T cells from LCMV-ARM infected mice using ATAC-seq (Buenrostro et al., 2013). The T cells were pre-sorted for KLRG1^{high} and KLRG1^{low} cells to segregate effector and memory-precursor populations. In both naive and post-infection T cells, among the prominent FOXO1-bound genomic sites were regulatory sequences of multiple AP-1 family members, including *Fos*, *JunB*, *FosB*, and *JunD* (Figure 1C). FOXO1 bound to open chromatin proximal to the TSS of each of these genes, or to nearby presumed enhancers (e. g., upstream of *Fos*) (Figure 1C). Found for both naïve and d12 P14 T cells, these data are consistent with FOXO1 acting as a direct or indirect co-repressor for genes that mediate T cell activation and differentiation (Im and Rao, 2004; Li et al., 2012). Thus, T cells that undergo *Foxo1* gene deletion immediately following thymic development constitutively display some, but not all, characteristics of activation.

Recently activated *Foxo1*-KO T cells exhibit similar AP-1 subunit levels, but decreased BACH2

Foxo1-KO cells exhibit an increased activation phenotype after infection (Hess Michelini et al., 2013; Utzschneider et al., 2018). Given the similar genomic binding of FOXO1 to AP-1 family members at day 0 vs. day 12 post-infection, we anticipated that we would observe increased AP-1 factors following infection: our working hypothesis was that FOXO1 was acting as a direct transcriptional co-repressor of AP-1 subunits. Instead, we observed similar AP-1 subunit mRNA and protein abundance in both KLRG1^{low} and KLRG1^{high} P14 cells at 7 days post-activation (Figures 2A, FigureS2A-D). Thus, FOXO1 appeared not to directly regulate AP-1 subunit abundance at d7 post-activation, despite detectable *Foxo1* mRNA (Figure S2E), and unambiguous genomic binding and regulation of known FOXO1 targets that include *Tcf7*, *Ccr7* and *Sell* (Figures S2F, G).

A parallel molecular mechanism attenuating AP-1 activity is the BACH2 transcriptional repressor: a key regulator of quiescence. BACH2 binds to a subset of AP-1 sites effectively blocking transactivation by AP-1 of proximal target genes (Roychoudhuri et al., 2016; Richer et al., 2016). We found FOXO1 exhibited genomic binding within, and proximal to, the *Bach2* gene locus at multiple sites in naive and day 12 post-infection cells (Figure 2B). We observed that *Bach2* becomes FOXO1-dependent only post-activation. Whereas naive WT and *Foxo1*-KO cells had similar, abundant *Bach2* mRNA expression, 7d and 12d post-activation WT cells exhibited a ~4-fold increase versus *Foxo1*-KO cells, in both KLRG1^{low} and KLRG1^{high} subsets (Figure 2C). As such, we predicted the target genes of AP-1 to be induced in BACH2-KO T cells.

The downstream activity of AP-1 homo- and heterodimers depends on the cell-type and the exact AP-1

factors under analysis. Among myriad AP-1 targets, several are genes encoding subunits of the AP-1 factors themselves (Angel et al., 1988; van Dam et al., 1993; Gazon et al., 2017). To examine whether AP-1 target gene expression would respond to deletion of the *Bach2* gene, we analyzed data comparing WT and *Bach2*-KO CD8^{+} naïve and T cells activated for 6 hours (Figure 2D; primary data from GSE77857 (Roychoudhuri et al., 2016)). In naïve T cells, the family of AP-1 genes (including NFAT paralogs (Rao et al., 1997)) were largely unaffected by the loss of *Bach2* (Figure 2D-left). In contrast, 6 hours after activation, AP-1 family genes were strongly increased in *Bach2*-KO relative to WT T cells (Figure 2D-right). Taken together, these observations are consistent with the idea that in the period immediately following activation, the modulation of T cell activation switches from a direct regulation of AP-1 genes by FOXO1 to a FOXO1 induction of the *Bach2* transcript and the resulting competition of BACH2 for AP-1 sites.

Activation of FOXO1 or inhibition of JNK dampens CD8^{+} T cell effector pathways

To address the phenotypic effects resulting from the absence of FOXO1 and the corresponding overexpression or overactivity of AP-1, we sought to measure T cell proliferation and the expression of effector functions. AP-1 can promote the expression of cytotoxic effector molecules, such as GZMB (Hanson et al., 1993; Babichuk and Bleackley, 1997) and pro-inflammatory cytokines such as IFNγ (Cippitelli et al., 1995; Zhang et al., 1998). Since FOXO1 exerts inhibitory influences on AP-1 expression in pre-activation naive cells (Figure 1), we explored the possibility that enforced nuclear expression of FOXO1 might have an opposite effect, that is, to suppress AP-1 and hence diminish the expression of genes encoding effector molecules. Furthermore, if these effects were working as a result of AP-1 modulation, we wished to test the prediction that inhibition of Jun-N-terminal kinase (JNK), capable of phosphorylating JUN and ATF family members, would also enhance T cell proliferation, and reduce the expression of the effector molecules, GZMB and IFNγ.

T cells from WT, *Foxo1*-KO and *Foxo1*-AAA mice were activated in culture via anti-CD3 and anti-CD28, and cellular divisions were measured with or without a Jun-N-terminal Kinase (JNK) inhibitor (JNKi) (Hibi et al., 1993; Barr et al., 2002) (Figures 3A,B). Compared with WT, T cells from *Foxo1*-KO mice displayed a diminished number of cell divisions, although T cells from *Foxo1*-AAA mice also displayed a modest but significant inhibition of recorded divisions. Consistent with a contribution of AP-1 to these phenotypic effects, a JNKi was able to enhance the number of cell divisions carried out by WT and *Foxo1*-KO T cells, and yet it did not affect the proliferation of *Foxo1*-AAA T cells that should exhibit AP-1 repression.

We assessed the expression of effector-associated GZMB in WT, *Foxo1*-KO, and *Foxo1*-AAA CD8^{+} T cells activated *in vitro*. Compared with WT T cells, *Foxo1*-KO T cells uniformly expressed higher amounts of GZMB, whereas in *Foxo1*-AAA T cells GZMB expression was reduced close to background levels (Figure 3C). Contrasting with its enhancement of proliferation, JNKi decreased the amount of GZMB expressed in both WT and *Foxo1*-KO T cells, and again it had no consistent effect on *Foxo1*-AAA T cells, where AP-1 is already suppressed (Figure 3D). To examine cytokine expression, we re-stimulated previously activated cultures with PMA plus ionomycin in the presence of a golgi transport inhibitor, and again, *Foxo1*-KO T cells displayed an

enhanced proportion of IFNγ-positive T cells along with an increased amount of IFNγ/cell among IFNγ$^+$ cells, compared with WT. Conversely, the proportion of IFNγ$^+$ T cells and the amount of IFNγ/cell was diminished in *Foxo1*-AAA T cells compared with WT (Figure 3E). In all cases, effector molecule or cytokine expression was highest in the *Foxo1*-KO, moderate in WT, and lowest in *Foxo1*-AAA T cells. Finally, similar to the results obtained for GZMB, both the proportion of IFNγ$^+$ T cells, and the amount of IFNγ expressed per cell were inhibited by JNKi (Figure 3F). These results are consistent with a role for FOXO1 in the inhibition of effector function. As we showed that FOXO1 supports suppression of AP-1 mRNA and protein, and direct suppression of AP-1 through JNK inhibition causes similar effects, we conclude that FOXO1 regulates effector vs. memory differentiation, in part, through its role in attenuating AP-1 expression.

FOXO1 diminishes effector molecule expression and increases CD127^{high} cells.

Previous studies showed that an acute loss of FOXO1 function just before or at the time of infection resulted in a substantial skewing of the T cell anti-viral response toward an effector phenotype represented by expression of KLRG1 and GZMB (Hess Michelini et al., 2013; Delpoux et al., 2017). We thus sought to determine how antigen-specific, *Foxo1*-AAA T cells respond a viral pathogen *in vivo* and accordingly regulate effector molecules. For this study we performed a mixed adoptive transfer of WT P14 and *Foxo1*-AAA P14 T cells into WT hosts, infected the hosts with LCMV-ARM, and tracked the abundance and phenotype of WT P14 and *Foxo1*-AAA P14 T cells. The analysis showed a ~20-fold defect in the accumulation of *Foxo1*-AAA P14 T cells relative to WT (Figures. 4A,B). The origin of this difference is consistent with reduced survival and the number of cells in cycle as measured by a decrease in BCL2 and Ki67 expression (Figure S3).

To determine whether *Foxo1*-AAA expression alters the differentiation decision between effector and memory precursor cells, we measured the expression of CD127 and KLRG1, where CD127$^+$KLRG1$^-$ cells are associated with a memory-precursor fate, and CD127$^-$KLRG1$^+$ cells are associated with a terminal effector fate (Kaech and Wherry, 2007). The results showed a two-fold increase in the proportion of CD127$^+$KLRG1$^-$ *Foxo1*-AAA cells at day 7, and a more modest difference in later time-points suggesting that enforced nuclear FOXO1 expression skews responding cells toward a memory precursor fate (Figure 4C). FOXO1 has also been shown to play a role in the inhibition of TBET expression, a regulator central to effector cell programming (Kerdiles et al., 2010; Rao et al., 2012; Luo and Li, 2018), and thus, *Foxo1*-AAA would be predicted to diminish TBET expression post-activation. To avoid confounding the results with the skewing of KLRG1 subsets, we first gated on KLRG1^{low} P14 cells since TBET is known to positively correlate with KLRG1 expression in WT cells. Even within the KLRG1^{low} population, we found *Foxo1*-AAA cells expressed lower amounts of TBET than WT controls (Figure 4D). These data are consistent with decreased KLRG1^{high} differentiation in *Foxo1*-AAA cells, and with the role of FOXO1 in skewing T cell differentiation toward a central memory phenotype.

Similarly, the expression of GZMB and IFNγ effector molecules was also affected by enforced nuclear expression of FOXO1. Paired sample plotting allowed a comparison between GZMB expression from WT and *Foxo1*-AAA P14 T cells from the same host animal (Figures 4E,F). These data reprised our *in vitro*

experiments—WT virus-specific CD8$^+$ T cells expressed higher GZMB and IFNγ than *Foxo1*-AAA virus-specific CD8$^+$ T cells. This, in turn, translated into fewer polyfunctional effector cells as measured by the co-expression of IFNγ and TNF (Figure 4G). These results are consistent with a role for FOXO1 in the inhibition of effector function. As we showed that FOXO1 supports suppression of AP-1 mRNA and protein, and direct suppression of AP-1 through JNK inhibition causes similar effects, we conclude that FOXO1 regulates effector vs. memory differentiation, in part, through its role in AP-1 expression.

Differential genomic accessibility in *Foxo1*-KO cells reflect increased effector and AP-1 signatures

We investigated transcription factor motifs found within sites of differential genomic accessibility in WT P14 and *Foxo1*-KO P14 T cells, before and after acute infection. Whereas some transcription factor motifs appeared with high frequency in these sites independent of genotype (including CTCF, CTCFL/BORIS, ETS, and RUNX factors; not shown), we found WT cells showed increases in Forkhead domain binding sites, presumably associated with opening of chromatin in the presence of FOXO1 (Figure S4A). In contrast, sites with increased genomic accessibility in *Foxo1*-KO T cells relative to WT exhibited increased binding sites for PRDM1 (BLIMP1), TBOX (TBET and EOMES), AP-1/BATF, and IRF factors—all important for development of effector function. As we have shown increased AP-1 abundance and decreased BACH2 in *Foxo1*-KO T cells relative to WT, the increased DNA accessibility in sites containing AP-1 binding sites suggest either: (1) increased AP-1 autoregulation, caused by FOXO1 deletion, results in increased chromatin accessibility proximal to AP-1 genes or, (2) an undetermined aspect of FOXO1 deletion possibly reflecting its ability to recruit co-repressors.

We and others have found increased TBET mRNA and protein in *Foxo1*-KO T cells (Kerdiles et al., 2010; Rao et al., 2012; Hess Michelini et al., 2013; Kim et al., 2013), and further, that graded expression of FOXO1 can be directly correlated with TCF7 expression and inversely correlated with TBET (Delpoux et al., 2017). Therefore, an increased number of TBOX-consensus binding sites within areas of differential DNA accessibility in *Foxo1*-KO vs. WT mice is consistent with the role of FOXO1 in suppressing TBET activity and inhibiting terminal effector T cell differentiation. Altogether, these data are consistent with *Foxo1*-WT cells possessing increased open chromatin near memory-associated transcription factors (i.e. Forkhead and HMG-box), but relatively decreased chromatin accessibility near effector-associated molecules (i.e. TBOX) in relation *Foxo1*-KO T cells.

The informatic analysis above renewed our interest in FOXO1 regulation of *Bach2*. In Figure 2C we reported decreased *Bach2* mRNA in *Foxo1*-KO post-activation CD8$^+$ T cells; to further investigate this, we obtained the RNA-seq data from a study of activated T cells from *Bach2*-KO mice (Roychoudhuri et al., 2016), and plotted a fold-change by fold-change plot of *Foxo1*-KO vs WT and *Bach2*-KO vs WT (Figure S4B). This plot revealed that *Foxo1* and known FOXO1 target *Tcf7* (Hess Michelini et al., 2013) were minimally regulated in *Bach2*-KO vs WT T cells. However, effector molecules *Gzma* and *Gzmb* were more abundant in *Foxo1*-KO and *Bach2*-KO T cells. We then re-examined our FOXO1 ChIP-seq data (Figures 1C, 2B), and found abundant individual FOXO1 binding sites in and near the *Bach2* gene locus, with peak calling software ascribing 13

FOXO1 genomic binding sites (the 7th most-abundantly-bound gene) in naïve cells and 8 FOXO1 binding sites (the 12th most-abundantly-bound gene) in day 12 post-infection CD8$^+$ P14 cells (Figures S4C, D). The binding sites nearest the gene locus are depicted in Figure 2B. Taken together, the above analysis is consistent with FOXO1 directly binding to the gene locus and nearby enhancers and positively regulating *Bach2* mRNA/protein abundance. This, in turn, regulates effector molecules, such as GZMB, likely through binding of AP-1 sites as previously reported (Roychoudhuri et al., 2016)).

Loss of FOXO1 expression leads to chronic activation in T cells surviving virus-infection

As previously presented, WT T cells and T cells acutely deleted for *Foxo1* initially expand with the same kinetics in response to infection with LCMV-ARM (Figure 5A). However, at 30 days post infection, the number of *Foxo1*-KO T cells was diminished compared to WT. This is in part due to the observation that d30 post-infection there are few, if any, *Foxo1*-KO memory T cells with the ability to undergo reactivation and proliferation in response to an antigenic re-challenge (Hess Michelini et al., 2013). The population of *Foxo1*-KO T cells 30 days post-infection displayed higher amounts of FOS, JUNB, and FOSB (Figure 5B). This presented the possibility that FOXO1-deficient cells are unable to completely regain quiescence and may exhibit signs of chronic activation that could lead to a state of exhaustion or senescence as described for chronically activated T cells in human beings (Plunkett et al., 2005; Chapman and Chi, 2018).

To assess this issue, we sought to examine the physiology of long-lived T cells subsequent to virus infection, especially that associated with chronic activation: increased frequency of apoptosis, evidence of activation, loss of co-receptor expression, an inability to produce multiple effector cytokines, or the induction of multiple inhibitory receptors (Effros, 1997; Parish et al., 2010). Apoptosis was examined by the presence of a cleaved and activated form of CASP3 (ActCASP3). Within CD44$^-$ naïve T cells there was a significant increase in the steady-state number of ActCASP3$^+$ cells with the loss of *Foxo1*, and such an increase was even more substantial in the d30 population of T cells with a memory-like KLRG1^{low} phenotype (Figure 5C). Strikingly, a similar result was found for the expression of CD69 as an indication of cellular activation. Whereas there was an approximately 3-fold increase in the number of CD69$^+$ *Foxo1*-KO naïve T cells compared to WT, the proportion of *Foxo1*-KO, KLRG1$^-$ memory-like T cells that continued to express CD69 was increased by approximately 15-fold over that of WT (Figure 5D).

Further analysis of day 30 T cells showed that within the population of KLRG1$^-$ T cells, few were Ki67$^+$, and yet there was a large population that sustained expression of granzyme B (Figures S5A, B). In addition, the number of T cells that remained capable of IFNγ production was increased in the absence of *Foxo1* (Figure S5C).

One hallmark of exhaustion as defined for T cells from mice or human beings infected with a persistent virus is the expression of the inhibitory receptors (Wherry et al., 2007; Wherry and Kurachi, 2015). Despite the high expression of CD69 and AP-1 at d30 post-infection, there was a virtually undetectable number of *Foxo1*-KO T cells that expressed in PD-1, LAG-3 or TIM3 (Figure S5D). This would seem to separate the concept of

"exhaustion" associated with receptor-based inhibitory signaling from the form of chronic activation exhibited by *Foxo1*-KO T cells. Rather, T cells that lack *Foxo1* appear to have characteristics of end-stage effector cells. They include a greater proportion of cells expressing CX3CR1 (fractalkine receptor) (Böttcher et al., 2015) (Figure S5E), and reduced proportion expressing CD27, the loss of which is characteristic of fully differentiated effector T cells (Grant et al., 2017) (Figure S5F).

A concept that is associated with chronic infections, cancer or autoimmunity in human beings is T cell replicative senescence. It is most consistently characterized by the loss of CD28 in both CD4 and CD8 T cells, but in addition, it can include defects in replication, shortened telomeres and elevated production of inflammatory cytokines (Vallejo, 2005; Henson et al., 2012; Chou and Effros, 2013). In *Foxo1*-KO T cells, CD28 was uniformly reduced in naïve T cells, and even it was more reduced in P14 *Foxo1*-KO KLRG1^{low} d30 p.i. T cells, compared with WT (Figure 5E). A further indication of senescence is the inability of T cells to produce effector cytokines: TNF, IFNγ, and IL-2. This was first measured as the proportion of cytokine-expressing T cells (positive for TNF, IFNγ, or both), and was found to be diminished in T cells from *Foxo1*-KO mice compared with WT (Figure 5F). Furthermore, the ability to simultaneously produce multiple cytokines, especially TNF, IFNγ, and IL-2 is a property of functional memory T cells, and as depicted in Figure 5G, *Foxo1*-KO mice possessed proportionately fewer double- and triple-cytokine producing T cells. These data indicate that FOXO1 is required to stave off the onset of a phenotypic unresponsiveness in T cells that is similar to that found in elderly human beings, especially in those T cells specific for chronic viruses such as human cytomegalovirus (Henson et al., 2012; Chou and Effros, 2013).

Expression of FOXO1 inversely correlates with a senescent phenotype acquired with age

In order to determine whether the effects of aging T cells are manifest in the expression of FOXO1, we sought to analyze T cells derived from human subjects of different ages. Human CD8$^+$ T cells can be classified through the expression of CD45RA and CD27 (Hamann et al., 1997; Kern et al., 1999; Sallusto et al., 1999): naïve, T_N: CD45RA$^+$ CD27$^+$; central memory T_{CM}: CD45RA$^-$ CD27$^+$; effector memory, T_{EM}: CD45RA$^-$ CD27$^-$; and effector memory that have re-expressed CD45RA, T_{EMRA}: CD45RA^{int} CD27$^-$. Most of the T_{EMRA} cells also express CD57 and KLRG1, and these are indicators of senescence (Brenchley, 2002) (Figure 6A). Each of the described CD8$^+$ T cell subsets was characterized for FOXO1 expression, and as shown, there was a clear hierarchy. T_N expressed the most FOXO1 followed by T_{CM}, T_{EM}, and senescent T_{EMRA} cells (Figure 6B).

TCF7 is a transcription factor that is essential for the formation of memory T cells and its expression is part of a program of gene expression that is predictive of CD8$^+$ T cells that will respond to chronic viral infections(Utzschneider et al., 2016; Wu et al., 2016; Lin et al., 2016) or tumors following checkpoint therapy (Zhou et al., 2010; Jeannet et al., 2010; Sade-Feldman et al., 2018; McLane et al., 2019; Siddiqui et al., 2019). Importantly, it is wholly dependent on FOXO1 for expression in mouse CD8$^+$ T cells post-activation(Hess Michelini et al., 2013), and as such, it showed the very same hierarchy of expression $T_N > T_{CM} > T_{EM} > T_{EMRA}$ (Figure 6C). A further comparison was carried out to examine the possibility that with diminished FOXO1 and TCF7 expression, AP-1 expression would be increased. The results showed that FOS and FOSB were

clearly expressed in higher amounts in senescent compared to naïve T cells, although this did not appear to be true for JUNB (Figure 6D).

To explore a connection between T cell senescence and aging, a comparison was made between blood from neonates (umbilical cord), healthy young adults, and elderly volunteers. In the representative example shown, CD8$^+$ T cells from neonates were entirely contained within T$_N$ and T$_{CM}$ subsets, young adults acquired T$_{EM}$ and T$_{EMRA}$ subsets, and the elderly possessed predominantly T$_{EMRA}$ cells (Figure 6E). Looking at the amount of FOXO1 expression CD8$^+$ T$_N$ cells, there was a strong and linear negative correlation between FOXO1 abundance and age (Figure 6F), and again, the very same correlation was found for TCF7 (Figure 6G). The inverse of these correlations was seen for FOS and FOSB but, again, not JUNB. Looking at young vs. elderly donor T$_N$ cells, there was a significant increase in the FOS family factors (Figure 6H).

Laboratory mice are considered "old" for aging studies between 18-24 months (equivalent in human beings is 56-69 y) (Flurkey et al., 2007; Weon and Je, 2012); however, specific pathogen-free (SPF) aged mice cannot be considered an accurate model for aged, disease-experienced, vaccinated human beings. Nonetheless, we wanted to examine whether T cells from aged SPF mice would recapitulate some of the hallmarks of aged, senescent cells that were observed in human beings. We observed a decrease in FOXO1 gMFI in naïve T cells from old mice vs. young mice (Figure S6A), although the changes in amounts of AP-1 in naïve T cells were only marginally affected (Figure S6B). However, there was a substantial and significant decrease in CD62L^{hi} (CD8$^+$CD44$^-$) T cells along with an increase in CD69 expression and a decrease in CD28 expression (Figures S6C-E)—all correlates of T cell senescence. Similarly, the number of naïve CD8$^+$ T cells in cycle was reduced (Figure S6F). These data recapitulate the key findings from the human studies—that naïve (CD44^{low}) T cells from older mice express less FOXO1 and more of two of the three AP-1 factors tested.

In summary, there is an age-dependent loss of FOXO1 and TCF7 expression and an increase in FOS expression that correlates in human CD8$^+$ T cells with the appearance of T$_{EMRA}$ cells at the expense of T$_N$ and T$_{CM}$ cells. Along with our analysis of a loss-of-function and constitutively-active mutations in mice, these data reveal a role for FOXO1 in suppressing T cell activation in part by attenuation of AP-1 factors, allowing maintenance of naïve and memory T cells in a state of antigen responsiveness.

Discussion

T cells are integral to organismal homeostasis. If they are diminished in function or number, commensal and infectious microbial and viral agents are overly virulent (as in AIDS), and yet, T cells are intrinsically capable of injuring their host. As such, the induction of T cell effector function is balanced on a knife-edge and regulated by strong and elaborate negative feedback control. FOXO transcription factors have been found to be essential to many aspects of adaptive immunity(Ouyang and Li, 2011; Hedrick et al., 2012), and it particular, they allow antigen-activated and expanded CD8$^+$ T cells to maintain stem cell-like qualities of self-renewal (Rao et al., 2012; Hess Michelini et al., 2013; Kim et al., 2013). In this report we show that FOXO1 is continually required to prevent or suppress a state of activation in naïve and post-activation CD8$^+$ T cells,

respectively, and in so doing, prevent the onset of senescence in the CD8$^+$ T cell population. The mechanism is, in part, the active suppression the AP-1 transcription factors, factors known to be central to many signaling pathways important for immune system activation(Foletta et al., 1998; Wisdom, 1999; Shaulian and Karin, 2002b).

These genetic data observed in mice have a correlate with the natural progression of T cell differentiation. Human T cells lose stem cell qualities with antigen-mediated activation as they progress from naïve T cells (CD27$^+$CD45RA^{high}) and central memory (CD27$^+$CD45RA$^-$) T cells to effector memory (CD27$^-$CD45RA$^-$) T cells and finally acquire a T_{EMRA} phenotype that exhibits intermediate expression of CD45RA, a lack of CD27, and strong expression of CD57 and KLRG1(Goronzy and Weyand, 2019). The data presented here indicate that the step-wise loss of "stemness" is inversely correlated with FOXO1 in control of TCF7 expression. Moreover, in comparing naïve to T_{EMRA} cells, an increase in the expression of two AP-1 subunits, FOS and FOSB was observed, although curiously, not JUNB.

This progression: $T_N \rightarrow T_{CM} \rightarrow T_{EM} \rightarrow T_{EMRA}$ also correlates with aging, as cord blood almost entirely consisted of naïve T cells, young adult blood contained approximately equivalent proportions of all four subsets, and blood from old subjects was largely made up of T_{EMRA} cells. Even cells meeting the commonly used definition of naïve human T cells, CD45RA$^+$CD27$^+$, displayed a decrease in FOXO1 and TCF7 with age of the donor. We conclude that the appearance of a senescent phenotype correlates with reduced FOXO1 and corresponding changes in TCF7 and certain AP-1 subunits. We propose that, given the close association between the phenotypes we recorded in mouse and human cells, that the senescence phenotype in T cells is mechanistically dependent on the amount of FOXO1 expression. Although FOXO1 is negatively regulated by growth factors that cause phosphorylation and nuclear localization, other types of transcriptional or post-translation regulatory mechanisms may also contribute to its lack of abundance in aging T cells. Of interest is whether nutrient abundance or the resulting manifestations of obesity, stress, and chronic inflammation can affect the amount of FOXO1 and thus the progression of immune senescence.

Aging is slowed in nematodes and flies when insulin-like signaling is reduced, similar to the effects of calorie restriction, and this enhanced longevity originates from a lack of inhibitory FOXO phosphorylation and the resulting FOXO-regulated gene transcription(Burgering, 2008; Salih and Brunet, 2008). Remarkably, there are indications that a similar process is found in human beings; genome-wide association studies have revealed FOXO1 and FOXO3 to be the most prominent among a small number of genes associated with increased age at death or age at natural menopause (Lunetta et al., 2007; Li et al., 2009; Kenyon, 2010; Anselmi et al., 2009; Flachsbart et al., 2009; Willcox et al., 2008). Since FOXO transcription factors are prominently involved in the insulin signaling pathway and are known to control glucose metabolism in most, if not all organs, one idea is that, similar to nematodes and flies, the key to FOXO regulation of longevity resides in its control of energy utilization (Kousteni, 2012). However, FOXO transcription factors play roles in many other aspects of physiology including stress resistance, cell cycle progression, apoptosis and immunity (Hedrick et al., 2012; Martins et al., 2016). In addition, FOXO1 is important in the regulation of genes involved in maintaining pluripotency and characteristics of stem cells (Zhang et al., 2011). This is a pathway that most likely originated

early in metazoan evolution as FOXO was found to be key to the self-renewal of all three stem cell lineages in Hydra—an immortal cnidarian genus diverged from bilateral phyla on the order of 600 million years ago (Boehm et al., 2012).

If immune plasticity is a factor in the aging process (Xu and Larbi, 2017; Goronzy and Weyand, 2017), then these data imply that one of the many ways in which FOXO transcription factors may affect longevity could include the maintenance of an effective adaptive immune system. With a diminished number of T cells capable of serial reactivation and renewal, and thus a reduced antigen-reactive repertoire, the inflammation and stress induced by infectious agents or cancer may accelerate aging averaged over an entire population.

Acknowledgments

Author contributions

A.D., R.H.M., S.M.H. and A.L.D. conceived the study and analyzed data. A.D. and N.M. performed the experiments and analyzed data. SMQ-P and C.M. obtained and analyzed human samples. S.M.H. and A.L.D. wrote the manuscript. C.K. and R.H.M. performed ChIP-seq and ATAC-seq experiments. K.A.A. performed the RNA-seq experiments. K.K. and L.L. established the human cohort/provided blood samples. A.L.D. analyzed RNA-seq data, and A.L.D. and C.K. analyzed ATAC-seq and ChIP-seq data. All authors reviewed the manuscript.

Declaration of interests

The authors declare no competing interests.

FIGURE LEGENDS

Figure 1: FOXO1 limits naive CD8$^+$ T cell AP-1 family member expression.

(A) mRNA abundance (RNA-seq) of WT and *Foxo1*-KO naive CD8$^+$ T cells. Selected genes are labeled, including members of the AP-1 family. As indicated in legend, grey point color indicates no FOXO1 genomic binding detected at day 0; green indicates one or more peaks detected; the size of points indicates number of FOXO1 genomic binding sites nearest the gene TSS. **(B)** Intracellular immunostaining determination of indicated protein abundance in naive P14 cells of the indicated genotypes and CD44 expression level. **(C)** FOXO1 genomic binding (ChIP-seq) and chromatin accessibility (ATAC-seq) for select AP-1 subunits in naive and post-infection (LCMV-ARM) P14 T cells. *y*-axis maximum for all ATAC-seq is 75. For (B), data are averaged from three experiments with n = 3 mice per group per experiment. * $P < 0.05$; ** $P < 0.01$; *** $P < 0.001$; **** $P < 0.0001$; unpaired Student's *t* test was used and error bars represent mean ± SEM. Informatics experiments are from one biological sample per condition.

Figure 2: FOXO1 drives *Bach2* in post-activation CD8$^+$ T cells to regulate AP-1.

(A) Selected AP-1 family members RNA abundance from WT and *Foxo1*-KO naive CD8$^+$ T cells at indicated time points, in uninfected mice or at indicated time/population post-infection with LCMV-ARM. Size of points indicates number of FOXO1 genomic binding sites nearest the gene TSS. **(B)** FOXO1 genomic binding (ChIP-seq) and chromatin accessibility (ATAC-seq) in naive and post-infection (LCMV-ARM) P14 T cells. **(C)** *Bach2* expression in WT and *Foxo1*-KO CD8$^+$ T cells at indicated time points in naive or post-infection P14 cells. **(D)** WT and *Bach2* KO cells before and after activation (RNA-seq; primary data GSE77857).

Figure 3: FOXO1- and JNK-dependent control of CD8$^+$ T cell effector functions and proliferation in vitro.

(A-F) WT, *Foxo1*-KO, and *Foxo1*-AAA naive CD8$^+$ T cells were activated in culture through CD3 and CD28 and IL-2 for three days. **(A)** Bar graph depicting the average number of cellular divisions of each genotype after 3 days. **(B)** Histograms depicting the cell trace violet fluorescence for each genotype, with or without JNKi. Inset numbers represent the average number of cellular divisions. Bar graph (right) indicates the average number of cellular divisions for each genotype. **(C)** GZMB intracellular immunostaining of CD8$^+$ T cells for indicated genotypes. Bar graphs indicate the gMFI. **(D)** GZMB expression in vehicle or JNKi treated cells. **(E)** PMA/IONO stimulation of cells of indicated genotypes followed by intracellular cytokine staining for IFNγ. Bar plots represent percent of IFNγ$^+$ among CD44hi CD69$^+$ cells (left panel) and gMFI of IFNγ among IFNγ$^+$ (right panel). **(F)** IFNγ expression following PMA/IONO re-stimulation with or without JNKi. Percent of IFNγ$^+$ among CD44^{hi} CD69$^+$ cells (upper panel) and gMFI of IFNγ among IFNγ$^+$ (lower panel). (A-B) Data are cumulative from 5 experiments with n= 2 or 3 mice per group. (C) Data are cumulative from 4 experiments with n= 2 or 3 mice per group. (D-F) Data are cumulative from 3 (AAA) to 4 (WT and KO) experiments with n= 2 or 3 mice per group. * $P < 0.05$; ** $P < 0.01$; *** $P < 0.001$; **** $P < 0.0001$; unpaired (A, C, E) or paired (B, D, F) Student's *t* test were used and error bars represent mean ± SEM.

Figure 4: Nuclear expression of FOXO1 enforces stem cell-like properties characteristic of CD8$^+$ T cell memory cells.

(A-G) A mixed adoptive transfer of WT P14 and *Foxo1*-AAA P14 T cells into WT hosts at day -1, and infected with LCMV-ARM on day 0. **(A)** The number and **(B)** relative abundance (as a percent of the total CD8$^+$ T cells) of splenic WT P14 and *Foxo1*-AAA P14 cells. **(C)** Differentiation as measured by CD127 and KLRG1. **(D)** TBET immunostaining on KLRG1^{low} cells. **(E)** GZMB was determined by immunostaining *ex vivo*. **(F)** IFNγ gMFI in indicated cells after 4 hours of PMA/IONO re-stimulation *ex vivo*. **(G)** Bar graphs represent the percentage of TNF and IFNγ double-positive after stimulation with PMA / IONO for 4 hours. (A-E) Data are from two experiments with 5 mice per time point. (E-F) Data are from one representative experiment among two experiment with 5 mice per time point. * $P < 0.05$; ** $P < 0.01$; *** $P < 0.001$; **** $P < 0.0001$; paired Student's *t* test were used and error bars represent mean ± SEM.

Figure 5: Naive and memory *Foxo1*-KO CD8 T cell exhibit a senescent phenotype.

(A-F) Adoptive transfer of WT P14 and *Foxo1*-KO P14 T cells into WT hosts at day -1 and infected with LCMV-ARM on day 0. **(A)** Bar graphs depict the number of WT P14 and *Foxo1*-KO P14 cells at day 30 p.i. **(B)** AP-1 factor immunostaining was determined at day 30 p.i. for KLRG1^{low} WT and *Foxo1*-KO P14 cells. **(C)** Expression of KLRG1 and Act-caspase-3 by WT and *Foxo1*-KO P14 cells before and 30 days post-infection. **(D**) Expression of KLRG1 and CD69 by WT and *Foxo1*-KO P14 cells before and 30 days post-infection. **(E)** Expression of CD28 by WT and *Foxo1*-KO P14 cells 30 days post-infection. **(F)** The proportion of T cells expressing either TNF, IFNγ or both **(G)** Proportion of T cells expressing the indicated cytokines. Upper panel indicating the poly-functionality among KLRG1^{low} cells (d30), lower panel, naïve T cells. (A) Data are cumulative from 2 to 4 experiments with minimum n=3 mice per group and per time point. (B) Data are cumulative from 2 experiments with n=5 mice per group. (C-G) Data are cumulative from 2 experiments with minimum n=3 mice per group and per experiment. *$P < 0.05$; **$P < 0.01$; ***$P < 0.001$; ****$P < 0.0001$; paired (A–G) unpaired (C-G) Student's *t* test was used and error bars represent mean ± SEM.

Figure 6: Age-dependent, inverse correlation of FOXO1 and AP-1 subunit abundance in human T cells.

(A) Total CD8$^+$ T cells analyzed for CD27 and CD45RA (left panel). Senescent T cells (T$_{sncnt}$) analyzed by KLRG1 vs. CD57 expression (left). Representative data from young adult cohort (right). **(B)** FOXO1 abundance among different CD8$^+$ T cell subsets (as identified by gating in (A)); bar graph at right depicts FOXO1 expression across indicated number (dots) of biological replicates. **(C)** TCF7 abundance among different CD8$^+$ T cell subsets; bar graph at right depicts TCF7 expression across indicated number (dots) of biological replicates. **(D)** FOS, JUNB and FOSB abundance determined among naive and senescent CD8$^+$ T cells. Data derived from individual young adult patient samples. **(E)** Expression of CD27 and CD45RA from a representative of each age group: cord blood, young adult, and elderly. **(F)** Quantitation of FOXO1 among naive CD8$^+$ T cells in cord blood, young adult, and old adult blood samples. Curve depicts a linear regression

of FOXO1 expression vs. age of the patients for CD8$^+$ T cells. **(G)** Quantitation of TCF7 among naive CD8$^+$ T cells in cord blood, young adult, and old adult blood samples. Curve depicts a linear regression of TCF7 expression vs. age of the patients for CD8$^+$ T cells. **(H)** Quantitation of FOS, JUNB, FOSB (MFI) among naive CD8$^+$ T cells from young and old adult blood samples. Curves represent the linear regression AP-1 expression vs. age of the patients among naive CD8$^+$ T cells. (A-H) Data represent 5 independent samples per group. *$P < 0.05$; **$P < 0.01$; ***$P < 0.001$; ****$P < 0.0001$; paired Student's t test was used (B, C and D) unpaired Student's t test was used (F, G and H) and error bars represent mean ± SEM.

STAR Methods

Resource Availability

Lead Contact

Further information and requests for resources and reagents should be directed to lead contact, Stephen M. Hedrick (shedrick@ucsd.edu).

Materials Availability

Reagents are commercially available and/or contacts for all materials are listed in Key Resources Table.

Data and code availability

RNA-seq, ChIP-seq, and ATAC-seq data is available from NCBI GEO/SRA [Submitted to GEO 12/14/20; Accn# pending]

KEY RESOURCES TABLE

REAGENT or RESOURCE	SOURCE	IDENTIFIER
Antibodies		
Anti-FOXO1	Cell Signaling Technology	clone C29H4
Anti-FOXO1-phospho-256	Cell Signaling Technology	cat#9461
Anti-FOS	Cell Signaling Technology	clone 9F6
Anti-FOSB	Cell Signaling Technology	clone 5G4
Anti-JunB	Cell Signaling Technology	clone C37F9
Anti-TCF7	Cell Signaling Technology	clone C63D9
Anti-GZMB	BD Biosciences	clone MHGB05
Anti-Ki67	BD Biosciences	clone B56
Anti-IFNg	Thermo Fisher Scientific	clone XMG1.2
Anti-TNFa	Thermo Fisher Scientific	clone MP6-XT22
Anti-IL2	Thermo Fisher Scientific	clone JES6-5H4
Bacterial and Virus Strains		
LCMV-Armstrong	Expanded in house	(Dutko and Oldstone, 1983)
Biological Samples		
Donor human PBMC	Australian Red Cross / University of Melbourne	https://www.redcross.org.au https://www.unimelb.edu.au
Chemicals, Peptides, and Recombinant Proteins		
JNK inhibitor	Calbiochem	Cat# 420116; (Barr et al., 2002)
Deposited Data		
Chip-Seq, ATAC-seq, RNA-seq	https://www.ncbi.nlm.nih.gov /geo/	[Submitted to GEO; waiting for Accn#]
Experimental Models: Organisms/Strains		
Foxo1[f/f]	Ronald DePinho, present address, MD Anderson Cancer Center	(Paik et al., 2007)

Foxo1-AAA	Ming Li, Memorial Sloan-Kettering Cancer Center	(Ouyang et al., 2012)
dLck-Cre	Jackson Laboratories	(Zhang et al., 2005)
P14 TCR transgenic	Jackson Laboratories	(Pircher et al., 1989)
C57BL/6J	Jackson Laboratories	strain #000664
Software and Algorithms		
HOMER	http://homer.ucsd.edu/homer	(Heinz et al., 2010)
Galaxy Bioinformatics Server	https://usegalaxy.org	(Blankenberg et al., 2010; Giardine et al., 2005; Goecks et al., 2010)
Bowtie2	https://usegalaxy.org	(Langmead and Salzberg, 2012)
MACS2	https://usegalaxy.org	(Zhang et al., 2008)
Trim Galore	https://usegalaxy.org	http://www.bioinformatics.babraham.ac.uk/projects/trim_galore/
FastQ Groomer	https://usegalaxy.org	(Blankenberg et al., 2010)
FastQC	https://usegalaxy.org	http://www.bioinformatics.babraham.ac.uk/projects/fastqc/
HISAT2	https://usegalaxy.org	(Kim et al., 2015)
Cuffdiff2	https://usegalaxy.org	(Trapnell et al., 2013)

Experimental Model and Method Details

Mice and tamoxifen treatment

Mice of various genotypes were congenic with the inbred strain C57BL/6 either by backcrossing or by direct genetic manipulation of C57BL/6 embryos. Host mice for adoptive transfers were either C57BL/6J-CD45.1$^{+/+}$ or C57BL/6J-CD45.1.2. P14$^{+/-}$ TCR-transgenic CD8$^+$ T cells specific for LCMV gp33 bound to H2D^b (Pircher et al., 1989) are referred to as P14. *Foxo1*$^{f/f}$ mice were crossed to dLck-Cre (B6.Cg-Tg (Lck-icre)3779Nik/J) (Zhang et al., 2005) mice to generate *Foxo1*$^{f/f}$ dLck-Cre$^{+/-}$ mice (*Foxo1*-KO) or *Foxo1*$^{f/f}$ dLck-Cre$^{-/-}$ mice (WT). *Foxo1*-AAA$^{f/f}$ (Ouyang et al., 2012) mice were crossed with dLck-Cre$^{+/-}$ to generate *Foxo1*-AAA mice. For adoptive transfer experiments, these strains were again crossed to P14 mice to generate P14-*Foxo1*-AAA$^{f/f}$ dLck-Cre$^{+/-}$ and P14-*Foxo1*$^{f/f}$ dLck-Cre$^{+/-}$ mice. Mice were maintained in a specific pathogen-free vivarium. All experiments were carried out in accordance to the Institutional Animal Care and Use Committee of University of California, San Diego.

Adoptive transfers and infection

Single-cell suspensions of spleens were homogenized and passed through a 40 μm nylon cell strainer in HBSS (Gibco) supplemented with 2% fetal bovine serum (FBS), pelleted at 400 x g for 5 minutes, and re-suspended in ACK lysis buffer for five minutes before addition of HBSS/2% FBS media. Adoptive transfers of P14 cells (typically 1 x 10^4) were performed via ~200 μl tail vein injection. Acute infections were performed by injection of 2 x 10^5 pfu LCMV-ARM i.p.

Method Details

Immunofluorescent staining and flow cytometry

Surface staining was performed as previously described (Delpoux et al., 2017). Antibody staining was performed with anti-CD4 (RM4-5), anti-CD8α (53-6.7), anti-CD44 (IM7), anti-CD45.1 (A20), anti-CD45.2 (104), anti-CD62L (MEL-14), anti-CD69 (H1.2F3), anti-CD127 (A7R34), anti-KLRG1 (2F1); all from Thermo Fisher or Biolegend. Rabbit anti-mouse TCF7 (C63D9) and FOXO1 (C29H4) were used in both directly-conjugated and secondary staining variations. FOS (9F6), JUNB (C37F9) and FOSB (5G4) antibodies were from Cell Signaling Technologies. Granzyme B (MHGB05) and Ki-67 (B56) antibodies were from BD Biosciences. TBET (4B10) antibody was from BioLegend. Secondary Alexa Fluor 647 donkey anti-rabbit (Invitrogen) was used in some cases as a secondary antibody for detection of FOXO1, FOS, JUNB, FOSB and TCF7 staining. For intracellular staining, the FOXP3 Staining Buffer Set (Thermo Fisher) was used. Immunofluorescence was acquired on a Fortessa or Fortessa X-20 cytometer (BD Biosciences) and analyzed using FlowJo Software (BD Biosciences).

Immunoblotting for FOXO1 and pFOXO-S253

Splenic naïve CD8$^+$ T cells were purified from mouse spleen with Biolegend naive CD8$^+$ isolation kit following the manufacturer's instructions. 1x10^6 cells were plated *in vitro* with plate-bound anti-CD3 and anti-CD28 (2 µg/ml) for the indicated time. Lysates were prepared in RIPA buffer containing ROCHE cOmplete. CD45.1$^+$ cells were positively selected from the splenocytes of LCMV-ARM infected host mice on days 7 and 12 using mouse CD45.1 selection kit from Biolegend, and stimulated *in vitro* using PMA / IONO cocktail (Thermo Fisher) for the indicated time; lysates were prepared as above. 50 µg/ sample of total protein were resolved on NuPAGE 4-12% Bis-Tris pre-cast gels from Thermo Fisher Scientific (NP0321) and transferred to 0.45µm PVDF membrane, incubated overnight at 4°C with primary antibodies. Phospho-FoxO1 (CST; 1:1000; Ser256; cat#9461; note antibody is named for human phospho-site) and FoxO1 (CST; 1:1000; C29H4; cat #2880). b-tubulin (cat# 05-661; 1:1000; Millipore). Membrane was washed thrice with 1X TBS-Tween20 and incubated with HRP-conjugated secondary antibody (CST, 1:1000 dilution) for 1 hr at room temperature, before chemiluminescent ECL substrate (GE, cat# 34095) imaging on Bio-Rad ChemiDoc and images processed and quantified with Image J software.

Cytokine detection

To asses intracellular cytokine production, 2 x 10^6 splenocytes were cultured for 4h at 37°C with or without PMA/IONO and 10 µg/ml monensin (both Thermo Fisher). Cells were stained for surface markers. Cytofix/Cytoperm Staining Buffer Set (BD Bioscience) was used for fixation and permeabilization, followed by labeling with specific cytokine antibodies for IFNγ (XMG1.2), TNF (MP6-XT22) and IL-2 (JES6-5H4; all from Thermo Fisher).

In vitro assays

Where indicated, naive CD8$^+$ T cells were purified from total spleen cells with naive CD8$^+$ isolation kit (Stem-

Cell or Biolegend), stained with 5 μM of Cell-Trace violet (Thermo Fisher) for 20 min at 37°C followed FBS quench and two washes. 1×10^5 cells per well were plated in anti-CD3/anti-CD28 each (4μg/ml) with IL-2 (100U/ml) for 3 days at 37°C. Proliferation index = Log_2 (f), where f=CFSE MFI (in absence of stimulation)/CFSE MFI (in presence of stimulation) (Delpoux et al., 2012). In some wells, JNKi (JNK Inhibitor I, L-Form, Calbiochem) (Barr et al., 2002) was added to 10 μM; JNKi was also added during the 4 hr of cytokine stimulation after the 3 days of culture. For Active Caspase-3 detection, CaspGlow Kit (Thermo fisher) was used per manufacturer's instructions. Briefly, splenocytes were stained for surface markers as described above and cultured at 2×10^6 cells/well in complete media. 1μl of FITC-DEVD-FMK was added in 300 μl cells. Cells were washed twice and acquired. Anti-activated-caspase3 antibody was used (BD bioscience) with Foxp3 kit was used (Thermo Fisher).

ChIP-seq, RNA-seq, and ATAC-seq

FOXO1 ChIP-seq was performed as before with minor modifications (Lin et al., 2010). Briefly, 3×10^7 T cells were fixed for 5 to 10 minutes at room temp in 1% formaldehyde then resuspended in lysis buffer. Following adaptor ligation, the DNAs were size selected (200-300bp) by 8% PAGE and index primers added by PCR. Samples were purified by 8% PAGE and precipitated with ethanol. Sequencing was performed by the BIOGEM core at UC San Diego using an Illumina HiSeq 2000 sequencer (50 cycles), mapped to mm10 (Bowtie2), and peaks were called with MACS2 and/or HOMER; after manual inspection, artifactual peaks for mir101c, Rn4.5s, and Pisd-ps3 were removed from the dataset. Peak annotation and motif finding were performed with HOMER (Heinz et al., 2010), and visualized with the UCSC genome browser (Kent et al., 2002).

RNA-seq was performed after cellular isolation by MACS column (naive cells) or FACS (post LCMV-ARM) on total RNA processed using the Illumina Truseq Stranded mRNA library preparation kit followed by single-end 50bp sequencing. Reads were processed on the Galaxy (Blankenberg et al., 2010; Giardine et al., 2005; Goecks et al., 2010) server via: FASTQ Groomer, Trim Galore, FastQC, HISAT2 (Refseq mm10 mapping to known genes first), Cuffdiff2. *mir*, *Snora*, and *Snord* genes were removed before plotting.

Genome-wide measurement of chromatin accessibility and computational alignment of generated data were performed using ATAC-Seq as described (Buenrostro et al., 2013) on 10,000 Naive CD8$^+$ T cells and P14 KLRG1^{hi} or KLRG1^{low} *Foxo1* KO and WT at indicated days LCMV-ARM infection.

Human samples and immunostaining

Following informed consent, peripheral blood mononuclear cells (PBMC) were obtained from healthy donors (recruited from the Australian Red Cross Service). Sero-negative donors for HIV, HCV, HTLV and syphilis were used. The University of Melbourne Human Ethics Committee approved volunteer recruitment and procedures associated. Experiments followed the guidelines set by the Australian NHMRC Code of Practice. Young adult patients were 22-35 years of age, old adults were 60-89 years old. Buffy coats were received from the Australian Red Cross Service (16 – 18h after bleed) and transferred to 50mL tubes. Blood was diluted with RPMI in a 1:1 ratio and mixed. PBMC were isolated using density-gradient centrifugation Ficoll-Paque (GE

Healthcare) in 50mL tubes. Frozen PBMCs were thawed in pre-warmed RPMI complete media (RPMI 1640 with 10% FBS, penicillin-streptomycin-glutamine (Thermo Fisher) and 55 μM β-mercaptoethanol (Sigma), washed with RPMI and re-suspended as required for experiments, stained with live/dead discrimination Fixable Viability Dye Near-IR (Thermo Fisher), surface stained for 20 min at 4°C in PBS supplemented with 2% FBS and 2mM EDTA, using the following antibodies: CD3 (UCHT1), CD4 (RPAT4), CD14 (MΦP9), CD45RA (L48) from BD bioscience, and CD8α (RPA-T8), CD19 (HIB19), CD27 (O323) and CD57 (HCD57) from BioLegend. KLRG1 (13F12F2) antibody is from Thermo Fisher, fixed and permeabilized using the Cytofix / Cytoperm kit (BD), or nuclear permeabilization and intracellular staining with FOXP3 transcription factor staining kit (Thermo Fisher). The following intracellular antibodies were used for intracellular or nuclear staining: TCF7 (7F11A10, BioLegend), Rabbit anti-Human FOS (9F6), JUNB (C37F9), FOSB (5G4) and FOXO1 (C29H4) from Cell Signaling Technology. Secondary Alexa Fluor 647 Donkey anti-Rabbit IgG (Invitrogen) was used. Cells were fixed with paraformaldehyde (2% PFA) before sample acquisition.

Quantification and statistical analysis

Prism6 software (GraphPad) was used to analyze data by two-tailed unpaired or paired Student's t-test when appropriate. * $P < 0.05$; ** $P < 0.01$; *** $P < 0.001$; **** $P < 0.0001$ was considered significant. Data are presented as means ± SEM.

References

Angel, P., Hattori, K., Smeal, T., and Karin, M. (1988) The jun proto-oncogene is positively autoregulated by its product, Jun/AP-1. Cell, *55*, 875–885.

Anselmi, C.V., Malovini, A., Roncarati, R., Novelli, V., Villa, F., Condorelli, G., Bellazzi, R., and Puca, A.A. (2009) Association of the FOXO3A locus with extreme longevity in a southern Italian centenarian study. Rejuvenation Res, *12*, 95–104.

Babichuk, C.K., and Bleackley, R.C. (1997) Mutational analysis of the murine granzyme B gene promoter in primary T cells and a T cell clone. J. Biol. Chem., *272*, 18564–18571.

Barr, R.K., Kendrick, T.S., and Bogoyevitch, M.A. (2002) Identification of the critical features of a small peptide inhibitor of JNK activity. J. Biol. Chem., *277*, 10987–10997.

Blankenberg, D., Gordon, A., Von Kuster, G., Coraor, N., Taylor, J., Nekrutenko, A., and Galaxy, T. (2010) Manipulation of FASTQ data with Galaxy. Bioinformatics, *26*, 1783–1785.

Boehm, A.M., Khalturin, K., Anton-Erxleben, F., Hemmrich, G., Klostermeier, U.C., Lopez-Quintero, J.A., Oberg, H.H., Puchert, M., Rosenstiel, P., Wittlieb, J. et al. (2012) FoxO is a critical regulator of stem cell maintenance in immortal Hydra. Proc. Natl. Acad. Sci. U S A, *109*, 19697–19702.

Böttcher, J.P., Beyer, M., Meissner, F., Abdullah, Z., Sander, J., Höchst, B., Eickhoff, S., Rieckmann, J.C., Russo, C., Bauer, T. et al. (2015) Functional classification of memory CD8(+) T cells by CX3CR1 expression. Nat Commun, *6*, 8306.

Brenchley, J.M. (2002) Expression of CD57 defines replicative senescence and antigen-induced apoptotic death of CD8+ T cells. Blood, *101*, 2711–2720.

Brunet, A., Park, J., Tran, H., Hu, L.S., Hemmings, B.A., and Greenberg, M.E. (2001) Protein kinase SGK mediates survival signals by phosphorylating the forkhead transcription factor FKHRL1 (FOXO3a). Mol. Cell. Biol., *21*, 952–965.

Buenrostro, J.D., Giresi, P.G., Zaba, L.C., Chang, H.Y., and Greenleaf, W.J. (2013) Transposition of native chromatin for fast and sensitive epigenomic profiling of open chromatin, DNA-binding proteins and nucleosome position. Nat Methods, *10*, 1213–1218.

Burgering, B.M. (2008) A brief introduction to FOXOlogy. Oncogene, *27*, 2258–2262.

Burgering, B.M., and Kops, G.J. (2002) Cell cycle and death control: long live Forkheads. Trends Biochem. Sci., *27*, 352–360.

Calnan, D.R., and Brunet, A. (2008) The FoxO code. Oncogene, *27*, 2276–2288.

Chapman, N.M., and Chi, H. (2018) Hallmarks of T-cell exit from quiescence. Cancer Immunol Res, *6*, 502–508.

Chou, J.P., and Effros, R.B. (2013) T cell replicative senescence in human aging. Curr Pharm Des, *19*, 1680–1698.

Cippitelli, M., Sica, A., Viggiano, V., Ye, J., Ghosh, P., Birrer, M.J., and Young, H.A. (1995) Negative transcriptional regulation of the interferon-gamma promoter by glucocorticoids and dominant negative mutants of c-Jun. J. Biol. Chem., *270*, 12548–12556.

Delpoux, A., Lai, C.Y., Hedrick, S.M., and Doedens, A.L. (2017) FOXO1 opposition of CD8$^+$ T cell effector programming confers early memory properties and phenotypic diversity. Proc. Natl. Acad. Sci. U S A, *114*, E8865–E8874.

Delpoux, A., Michelini, R.H., Verma, S., Lai, C.Y., Omilusik, K.D., Utzschneider, D.T., Redwood, A.J., Goldrath, A.W., Benedict, C.A., and Hedrick, S.M. (2018) Continuous activity of Foxo1 is required to prevent anergy and maintain the memory state of CD8+T cells. J. Exp. Med., *215*, 575–594.

Delpoux, A., Poitrasson-Rivière, M., Le Campion, A., Pommier, A., Yakonowsky, P., Jacques, S., Letourneur, F., Randriamampita, C., Lucas, B., and Auffray, C. (2012) Foxp3-independent loss of regulatory CD4+ T-cell suppressive capacities induced by self-deprivation. Eur. J. Immunol., *42*, 1237–1249.

Dutko, F.J., and Oldstone, M.B. (1983) Genomic and biological variation among commonly used lymphocytic choriomeningitis virus strains. J. Gen. Virol., *64*, 1689–1698.

Effros, R.B. (1997) Loss of CD28 expression on T lymphocytes: a marker of replicative senescence. Dev Comp Immunol, *21*, 471–478.

Flachsbart, F., Caliebe, A., Kleindorp, R., Blanche, H., von Eller-Eberstein, H., Nikolaus, S., Schreiber, S., and Nebel, A. (2009) Association of FOXO3A variation with human longevity confirmed in German centenarians. Proc. Natl. Acad. Sci. U S A, *106*, 2700–2705.

Flurkey, K., Currer, J.M., and Harrison, D.E. (2007) The Mouse in Aging Research. In The Mouse in Biomedical Research 2nd Edition, J.G.E.A. Fox, ed. (Burlington, MA: Elsevier), pp. 637–672.

Foletta, V.C., Segal, D.H., and Cohen, D.R. (1998) Transcriptional regulation in the immune system: all roads lead to AP-1. J. Leukoc. Biol., *63*, 139–152.

Gazon, H., Barbeau, B., Mesnard, J.M., and Peloponese, J.M. (2017) Hijacking of the AP-1 Signaling Pathway during Development of ATL. Front Microbiol, *8*, 2686.

Giardine, B., Riemer, C., Hardison, R.C., Burhans, R., Elnitski, L., Shah, P., Zhang, Y., Blankenberg, D., Albert, I., Taylor, J. et al. (2005) Galaxy: a platform for interactive large-scale genome analysis. Genome Res., *15*, 1451–1455.

Goecks, J., Nekrutenko, A., Taylor, J., and Galaxy, T. (2010) Galaxy: a comprehensive approach for supporting accessible, reproducible, and transparent computational research in the life sciences. Genome Biol, *11*, R86.

Goronzy, J.J., and Weyand, C.M. (2017) Successful and Maladaptive T Cell Aging. Immunity, *46*, 364–378.

Goronzy, J.J., and Weyand, C.M. (2019) Mechanisms underlying T cell ageing. Nat Rev Immunol, *19*, 573–583.

Gottlieb, S., and Ruvkun, G. (1994) daf-2, daf-16 and daf-23: genetically interacting genes controlling Dauer formation in Caenorhabditis elegans. Genetics, *137*, 107–120.

Grant, E.J., Nüssing, S., Sant, S., Clemens, E.B., and Kedzierska, K. (2017) The role of CD27 in anti-viral T-cell immunity. Curr Opin Virol, *22*, 77–88.

Guertin, D.A., Stevens, D.M., Thoreen, C.C., Burds, A.A., Kalaany, N.Y., Moffat, J., Brown, M., Fitzgerald, K.J., and Sabatini, D.M. (2006) Ablation in mice of the mTORC components raptor, rictor, or mLST8 reveals that mTORC2 is required for signaling to Akt-FOXO and PKCalpha, but not S6K1. Dev. Cell, *11*, 859–871.

Gustafson, C.E., Cavanagh, M.M., Jin, J., Weyand, C.M., and Goronzy, J.J. (2018) Functional pathways regulated by microRNA networks in CD8 T-cell aging. Aging Cell, e12879.

Hamann, D., Baars, P.A., Rep, M.H., Hooibrink, B., Kerkhof-Garde, S.R., Klein, M.R., and van Lier, R.A. (1997) Phenotypic and functional separation of memory and effector human CD8+ T cells. J. Exp. Med., *186*, 1407–1418.

Hanson, R.D., Grisolano, J.L., and Ley, T.J. (1993) Consensus AP-1 and CRE motifs upstream from the human cytotoxic serine protease B (CSP-B/CGL-1) gene synergize to activate transcription. Blood, *82*, 2749–2757.

Hedrick, S.M., Hess Michelini, R., Doedens, A.L., Goldrath, A.W., and Stone, E.L. (2012) FOXO transcription factors throughout T cell biology. Nat Rev Immunol, *12*, 649–661.

Heinz, S., Benner, C., Spann, N., Bertolino, E., Lin, Y.C., Laslo, P., Cheng, J.X., Murre, C., Singh, H., and Glass, C.K. (2010) Simple combinations of lineage-determining transcription factors prime cis-regulatory elements required for macrophage and B cell identities. Mol. Cell., *38*, 576–589.

Henson, S.M., Riddell, N.E., and Akbar, A.N. (2012) Properties of end-stage human T cells defined by CD45RA re-expression. Curr. Opin. Immunol., *24*, 476–481.

Hess Michelini, R., Doedens, A.L., Goldrath, A.W., and Hedrick, S.M. (2013) Differentiation of CD8 memory T cells depends on Foxo1. J. Exp. Med., *210*, 1189–1200.

Hibi, M., Lin, A., Smeal, T., Minden, A., and Karin, M. (1993) Identification of an oncoprotein- and UV-responsive protein kinase that binds and potentiates the c-Jun activation domain. Genes Dev., *7*, 2135–2148.

Im, S.H., and Rao, A. (2004) Activation and deactivation of gene expression by Ca2+/calcineurin-NFAT-mediated signaling. Mol Cells, *18*, 1–9.

Jeannet, G., Boudousquie, C., Gardiol, N., Kang, J., Huelsken, J., and Held, W. (2010) Essential role of the Wnt pathway effector Tcf-1 for the establishment of functional CD8 T cell memory. Proc. Natl. Acad. Sci. U S A, *107*, 9777–9782.

Kaech, S.M., and Wherry, E.J. (2007) Heterogeneity and cell-fate decisions in effector and memory CD8+ T cell differentiation during viral infection. Immunity, *27*, 393–405.

Kent, W.J., Sugnet, C.W., Furey, T.S., Roskin, K.M., Pringle, T.H., Zahler, A.M., and Haussler, D. (2002) The human genome browser at UCSC. Genome Res., *12*, 996–1006.

Kenyon, C., Chang, J., Gensch, E., Rudner, A., and Tabtiang, R. (1993) A C. elegans mutant that lives twice as long as wild type. Nature, *366*, 461–464.

Kenyon, C.J. (2010) The genetics of ageing. Nature, *464*, 504–512.

Kerdiles, Y.M., Beisner, D.R., Tinoco, R., Dejean, A.S., Castrillon, D.H., DePinho, R.A., and Hedrick, S.M. (2009) Foxo1 links homing and survival of naive T cells by regulating L-selectin, CCR7 and interleukin 7 receptor. Nat Immunol, *10*, 176–184.

Kerdiles, Y.M., Stone, E.L., Beisner, D.R., McGargill, M.A., Ch'en, I.L., Stockmann, C., Katayama, C.D., and Hedrick, S.M. (2010) Foxo transcription factors control regulatory T cell development and function. Immunity, *33*, 890–904.

Kern, F., Khatamzas, E., Surel, I., Frömmel, C., Reinke, P., Waldrop, S.L., Picker, L.J., and Volk, H.D. (1999) Distribution of human CMV-specific memory T cells among the CD8pos. subsets defined by CD57, CD27, and CD45 isoforms. Eur. J. Immunol., *29*, 2908–2915.

Kim, D., Langmead, B., and Salzberg, S.L. (2015) HISAT: a fast spliced aligner with low memory requirements. Nat Methods, *12*, 357–360.

Kim, M.V., Ouyang, W., Liao, W., Zhang, M.Q., and Li, M.O. (2013) The transcription factor Foxo1 controls central-memory CD8+ T cell responses to infection. Immunity, *39*, 286–297.

Kousteni, S. (2012) FoxO1, the transcriptional chief of staff of energy metabolism. Bone, *50*, 437–443.

Langmead, B., and Salzberg, S.L. (2012) Fast gapped-read alignment with Bowtie 2. Nat Methods, *9*, 357–359.

Li, P., Spolski, R., Liao, W., Wang, L., Murphy, T.L., Murphy, K.M., and Leonard, W.J. (2012) BATF-JUN is critical for IRF4-mediated transcription in T cells. Nature, *490*, 543–546.

Li, Y., Wang, W.J., Cao, H., Lu, J., Wu, C., Hu, F.Y., Guo, J., Zhao, L., Yang, F., Zhang, Y.X. et al. (2009) Genetic association of FOXO1A and FOXO3A with longevity trait in Han Chinese populations. Hum. Mol. Genet., *18*, 4897–4904.

Liang, R., and Ghaffari, S. (2018) Stem Cells Seen Through the FOXO Lens: An Evolving Paradigm. Curr. Top. Dev. Biol., *127*, 23–47.

Lin, W.W., Nish, S.A., Yen, B., Chen, Y.H., Adams, W.C., Kratchmarov, R., Rothman, N.J., Bhandoola, A., Xue, H.H., and Reiner, S.L. (2016) CD8+ T Lymphocyte Self-Renewal during Effector Cell Determination. Cell Rep, *17*, 1773–1782.

Lunetta, K.L., D'Agostino, R.B.S., Karasik, D., Benjamin, E.J., Guo, C.Y., Govindaraju, R., Kiel, D.P., Kelly-Hayes, M., Massaro, J.M., Pencina, M.J. et al. (2007) Genetic correlates of longevity and selected age-related phenotypes: a genome-wide association study in the Framingham Study. BMC Med Genet, *8 Suppl 1*, S13.

Luo, C.T., and Li, M.O. (2018) Foxo transcription factors in T cell biology and tumor immunity. Semin. Cancer Biol., *50*, 13–20.

Martins, R., Lithgow, G.J., and Link, W. (2016) Long live FOXO: unraveling the role of FOXO proteins in aging and longevity. Aging Cell, *15*, 196–207.

McLane, L.M., Abdel-Hakeem, M.S., and Wherry, E.J. (2019) CD8 T Cell Exhaustion During Chronic Viral Infection and Cancer. Annu. Rev. Immunol., *37*, 457–495.

McLaughlin, C.N., and Broihier, H.T. (2018) Keeping Neurons Young and Foxy: FoxOs Promote Neuronal Plasticity. Trends Genet., *34*, 65–78.

Ouyang, W., and Li, M.O. (2011) Foxo: in command of T lymphocyte homeostasis and tolerance. Trends Immunol, *32*, 26–33.

Ouyang, W., Liao, W., Luo, C.T., Yin, N., Huse, M., Kim, M.V., Peng, M., Chan, P., Ma, Q., Mo, Y. et al. (2012) Novel Foxo1-dependent transcriptional programs control T(reg) cell function. Nature, *491*, 554–559.

Paik, J.H., Kollipara, R., Chu, G., Ji, H., Xiao, Y., Ding, Z., Miao, L., Tothova, Z., Horner, J.W., Carrasco, D.R. et al. (2007) FoxOs are lineage-restricted redundant tumor suppressors and regulate endothelial cell homeostasis. Cell, *128*, 309–323.

Parish, S.T., Wu, J.E., and Effros, R.B. (2010) Sustained CD28 expression delays multiple features of replicative senescence in human CD8 T lymphocytes. J. Clin. Immunol., *30*, 798–805.

Pircher, H., Burki, K., Lang, R., Hengartner, H., and Zinkernagel, R.M. (1989) Tolerance induction in double specific T-cell receptor transgenic mice varies with antigen. Nature, *342*, 559–561.

Plunkett, F.J., Franzese, O., Belaramani, L.L., Fletcher, J.M., Gilmour, K.C., Sharifi, R., Khan, N., Hislop, A.D., Cara, A., Salmon, M. et al. (2005) The impact of telomere erosion on memory CD8+ T cells in patients with X-linked lymphoproliferative syndrome. Mech Ageing Dev, *126*, 855–865.

Rao, A., Luo, C., and Hogan, P.G. (1997) Transcription factors of the NFAT family: regulation and function. Annu. Rev. Immunol., *15*, 707–747.

Rao, R.R., Li, Q., Gubbels Bupp, M.R., and Shrikant, P.A. (2012) Transcription Factor Foxo1 Represses T-bet-Mediated Effector Functions and Promotes Memory CD8(+) T Cell Differentiation. Immunity, *36*, 374–387.

Richer, M.J., Lang, M.L., and Butler, N.S. (2016) T Cell Fates Zipped Up: How the Bach2 Basic Leucine Zipper Transcriptional Repressor Directs T Cell Differentiation and Function. J. Immunol., *197*, 1009–1015.

Roychoudhuri, R., Clever, D., Li, P., Wakabayashi, Y., Quinn, K.M., Klebanoff, C.A., Ji, Y., Sukumar, M., Eil, R.L., Yu, Z. et al. (2016) BACH2 regulates CD8(+) T cell differentiation by controlling access of AP-1 factors to enhancers. Nat Immunol, *17*, 851–860.

Sade-Feldman, M., Yizhak, K., Bjorgaard, S.L., Ray, J.P., de Boer, C.G., Jenkins, R.W., Lieb, D.J., Chen, J.H., Frederick, D.T., Barzily-Rokni, M. et al. (2018) Defining T Cell States Associated with Response to Checkpoint Immunotherapy in Melanoma. Cell, *175*, 998–1013.e20.

Salih, D.A., and Brunet, A. (2008) FoxO transcription factors in the maintenance of cellular homeostasis during aging. Curr. Opin. Cell Biol., *20*, 126–136.

Sallusto, F., Lenig, D., Förster, R., Lipp, M., and Lanzavecchia, A. (1999) Two subsets of memory T lymphocytes with distinct homing potentials and effector functions. Nature, *401*, 708–712.

Shaulian, E., and Karin, M. (2002a) AP-1 as a regulator of cell life and death. Nat Cell Biol, *4*, E131–6.

Shaulian, E., and Karin, M. (2002b) AP-1 as a regulator of cell life and death. Nature Cell Biol., *4*, E131–E136.

Siddiqui, I., Schaeuble, K., Chennupati, V., Fuertes Marraco, S.A., Calderon-Copete, S., Pais Ferreira, D., Carmona, S.J., Scarpellino, L., Gfeller, D., Pradervand, S. et al. (2019) Intratumoral Tcf1+PD-1+CD8+ T Cells with Stem-like Properties Promote Tumor Control in Response to Vaccination and Checkpoint Blockade Immunotherapy. Immunity, *50*, 195–211.e10.

Stone, E.L., Pepper, M., Katayama, C.D., Kerdiles, Y.M., Lai, C.Y., Emslie, E., Lin, Y.C., Yang, E., Goldrath, A.W., Li, M.O. et al. (2015) ICOS coreceptor signaling inactivates the transcription factor FOXO1 to promote Tfh cell differentiation. Immunity, *42*, 239–251.

Tamahara, T., Ochiai, K., Muto, A., Kato, Y., Sax, N., Matsumoto, M., Koseki, T., and Igarashi, K. (2017) The mTOR-Bach2 Cascade Controls Cell Cycle and Class Switch Recombination during B Cell Differentiation. Mol. Cell. Biol., *37*,

Tejera, M.M., Kim, E.H., Sullivan, J.A., Plisch, E.H., and Suresh, M. (2013) FoxO1 controls effector-to-memory transition and maintenance of functional CD8 T cell memory. J. Immunol., *191*, 187–199.

Trapnell, C., Hendrickson, D.G., Sauvageau, M., Goff, L., Rinn, J.L., and Pachter, L. (2013) Differential analysis of gene regulation at transcript resolution with RNA-seq. Nat Biotechnol, *31*, 46–53.

Turner, R., and Tjian, R. (1989) Leucine repeats and an adjacent DNA binding domain mediate the formation of functional cFos-cJun heterodimers. Science, *243*, 1689–1694.

Utzschneider, D.T., Charmoy, M., Chennupati, V., Pousse, L., Ferreira, D.P., Calderon-Copete, S., Danilo, M., Alfei, F., Hofmann, M., Wieland, D. et al. (2016) T Cell Factor 1-Expressing Memory-like CD8(+) T Cells Sustain the Immune Response to Chronic Viral Infections. Immunity, *45*, 415–427.

Utzschneider, D.T., Delpoux, A., Wieland, D., Huang, X., Lai, C.Y., Hofmann, M., Thimme, R., and Hedrick, S.M. (2018) Active Maintenance of T Cell Memory in Acute and Chronic Viral Infection Depends on Continuous Expression of FOXO1. Cell Rep, *22*, 3454–3467.

Vallejo, A.N. (2005) CD28 extinction in human T cells: altered functions and the program of T-cell senescence. Immunol. Rev., *205*, 158–169.

van Dam, H., Duyndam, M., Rottier, R., Bosch, A., de Vries-Smits, L., Herrlich, P., Zantema, A., Angel, P., and van der Eb, A.J. (1993) Heterodimer formation of cJun and ATF-2 is responsible for induction of c-jun by the 243 amino acid adenovirus E1A protein. EMBO J., *12*, 479–487.

Van Der Heide, L.P., Hoekman, M.F., and Smidt, M.P. (2004) The ins and outs of FoxO shuttling: mechanisms of FoxO translocation and transcriptional regulation. Biochem. J., *380*, 297–309.

Weon, B.M., and Je, J.H. (2012) Trends in scale and shape of survival curves. Sci Rep, *2*, 504.

Wherry, E.J., Ha, S.J., Kaech, S.M., Haining, W.N., Sarkar, S., Kalia, V., Subramaniam, S., Blattman, J.N., Barber, D.L., and Ahmed, R. (2007) Molecular signature of CD8+ T cell exhaustion during chronic viral infection. Immunity, *27*, 670–684.

Wherry, E.J., and Kurachi, M. (2015) Molecular and cellular insights into T cell exhaustion. Nat Rev Immunol, *15*, 486–499.

Willcox, B.J., Donlon, T.A., He, Q., Chen, R., Grove, J.S., Yano, K., Masaki, K.H., Willcox, D.C., Rodriguez, B., and Curb, J.D. (2008) FOXO3A genotype is strongly associated with human longevity. Proc. Natl. Acad. Sci. U S A, *105*, 13987–13992.

Wisdom, R. (1999) AP-1: one switch for many signals. Exp Cell Res, *253*, 180–185.

Wu, T., Ji, Y., Moseman, E.A., Xu, H.C., Manglani, M., Kirby, M., Anderson, S.M., Handon, R., Kenyon, E., Elkahloun, A. et al. (2016) The TCF1-Bcl6 axis counteracts type I interferon to repress exhaustion and maintain T cell stemness. Sci Immunol, *1*,

Xu, W., and Larbi, A. (2017) Markers of T Cell Senescence in Humans. Int J Mol Sci, *18*,

Zhang, D.J., Wang, Q., Wei, J., Baimukanova, G., Buchholz, F., Stewart, A.F., Mao, X., and Killeen, N. (2005) Selective expression of the Cre recombinase in late-stage thymocytes using the distal promoter of the Lck gene. J. Immunol., *174*, 6725–6731.

Zhang, F., Wang, D.Z., Boothby, M., Penix, L., Flavell, R.A., and Aune, T.M. (1998) Regulation of the activity of IFN-gamma promoter elements during Th cell differentiation. J. Immunol., *161*, 6105–6112.

Zhang, P.F., Wu, J., Wu, Y., Huang, W., Liu, M., Dong, Z.R., Xu, B.Y., Jin, Y., Wang, F., and Zhang, X.M. (2019) The lncRNA SCARNA2 mediates colorectal cancer chemoresistance through a conserved microRNA-342-3p target sequence. J. Cell. Physiol., *234*, 10157–10165.

Zhang, X., Yalcin, S., Lee, D.F., Yeh, T.Y., Lee, S.M., Su, J., Mungamuri, S.K., Rimmele, P., Kennedy, M., Sellers, R. et al. (2011) FOXO1 is an essential regulator of pluripotency in human embryonic stem cells. Nat Cell Biol, *13*, 1092–1099.

Zhang, Y., Liu, T., Meyer, C.A., Eeckhoute, J., Johnson, D.S., Bernstein, B.E., Nusbaum, C., Myers, R.M., Brown, M., Li, W. et al. (2008) Model-based analysis of ChIP-Seq (MACS). Genome Biol, *9*, R137.

Zhou, X., Yu, S., Zhao, D.M., Harty, J.T., Badovinac, V.P., and Xue, H.H. (2010) Differentiation and persistence of memory CD8(+) T cells depend on T cell factor 1. Immunity, *33*, 229–240.

KEY RESOURCES TABLE

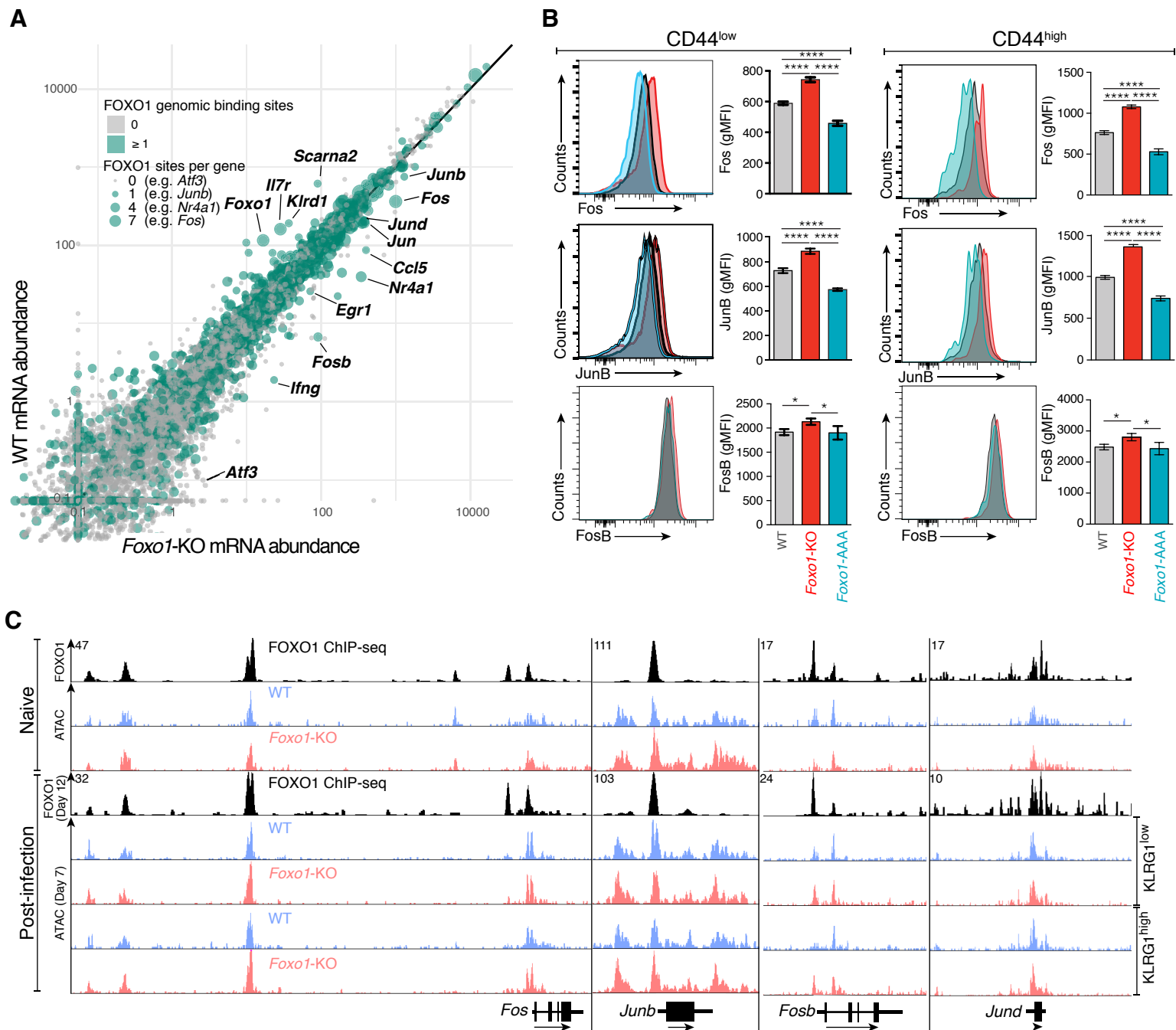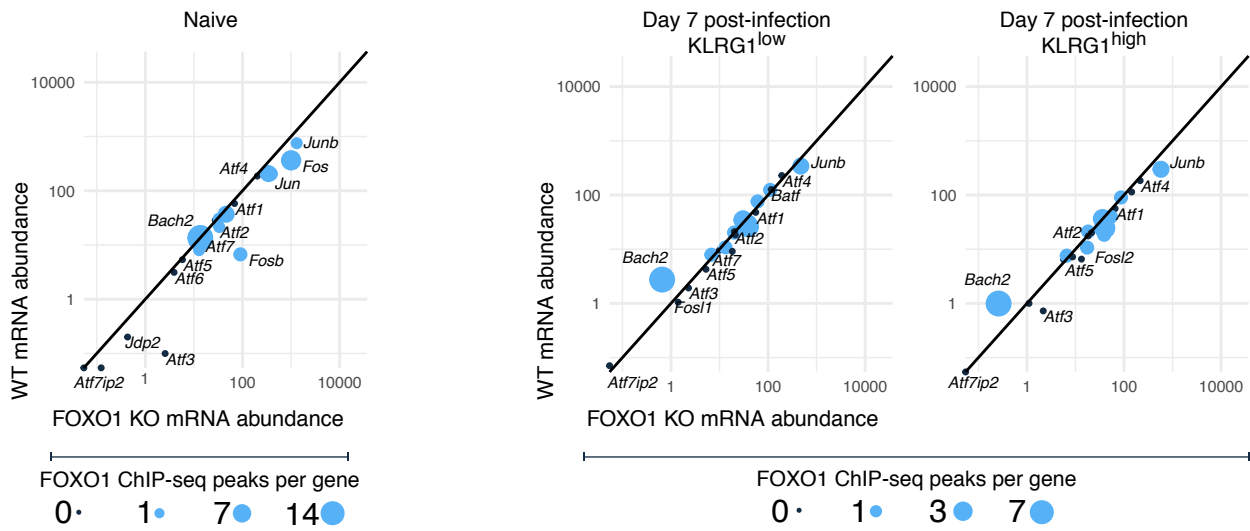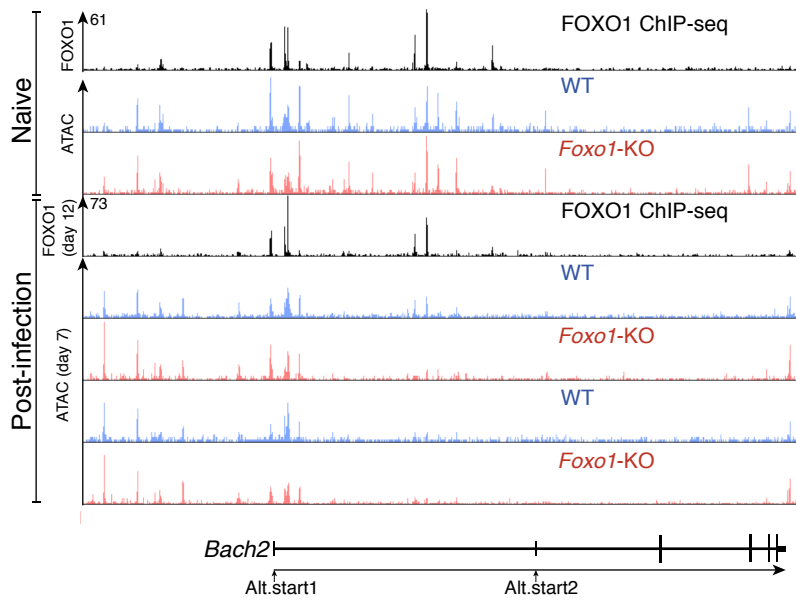| REAGENT or RESOURCE	SOURCE	IDENTIFIER
Antibodies		
Anti-FOXO1	Cell Signaling Technology	clone C29H4
Anti-FOXO1-phospho-256	Cell Signaling Technology	cat#9461
Anti-FOS	Cell Signaling Technology	clone 9F6
Anti-FOSB	Cell Signaling Technology	clone 5G4
Anti-JunB	Cell Signaling Technology	clone C37F9
Anti-TCF7	Cell Signaling Technology	clone C63D9
Anti-GZMB	BD Biosciences	clone MHGB05
Anti-Ki67	BD Biosciences	clone B56
Anti-IFNg	Thermo Fisher Scientific	clone XMG1.2
Anti-TNFa	Thermo Fisher Scientific	clone MP6-XT22
Anti-IL2	Thermo Fisher Scientific	clone JES6-5H4
Bacterial and Virus Strains		
LCMV-Armstrong	Expanded in house	(Dutko and Oldstone, 1983)
Biological Samples		
Donor human PBMC	Australian Red Cross / University of Melbourne	https://www.redcross.org.au https://www.unimelb.edu.au
Chemicals, Peptides, and Recombinant Proteins		
JNK inhibitor	Calbiochem	Cat# 420116; (Barr et al., 2002)
Deposited Data		
Chip-Seq, ATAC-seq, RNA-seq	https://www.ncbi.nlm.nih.gov/geo/	GEO Accn#
Experimental Models: Organisms/Strains		
FOXO1 floxed	Ronald DePinho, present address, MD Anderson Cancer Center	(Paik et al., 2007)
FOXO1-AAA	Ming Li, Memorial Sloan-Kettering Cancer Center	(Ouyang et al., 2012)
dLCK-Cre	Jackson Laboratories	(Zhang et al., 2005)
C57BL/6J	Jackson Laboratories	strain #000664
Software and Algorithms		
HOMER	http://homer.ucsd.edu/homer	(Heinz et al., 2010)
Galaxy Bioinformatics Server	https://usegalaxy.org	(Blankenberg et al., 2010; Giardine et al., 2005; Goecks et al., 2010)
Bowtie2	https://usegalaxy.org	(Langmead and Salzberg, 2012)
MACS2	https://usegalaxy.org	(Zhang et al., 2008)
Trim Galore	https://usegalaxy.org	http://www.bioinformatics.babraham.ac.uk/projects/trim_galore/
FastQ Groomer	https://usegalaxy.org	(Blankenberg et al., 2010)
FastQC	https://usegalaxy.org	http://www.bioinformatics.babraham.ac.uk/projects/fastqc/
HISAT2	https://usegalaxy.org	(Kim et al., 2015)
Cuffdiff2	https://usegalaxy.org	(Trapnell et al., 2013)

Figure 1

Figure 1 Delpoux et al.

A

FOXO1 genomic binding sites
- 0
- ≥ 1

FOXO1 sites per gene
- 0 (e.g. *Atf3*)
- 1 (e.g. *Junb*)
- 4 (e.g. *Nr4a1*)
- 7 (e.g. *Fos*)

WT mRNA abundance

Foxo1-KO mRNA abundance

Scarna2, *Il7r*, *Foxo1*, *Klrd1*, *Junb*, *Fos*, *Jund*, *Jun*, *Ccl5*, *Nr4a1*, *Egr1*, *Fosb*, *Ifng*, *Atf3*

B

CD44^low

CD44^high

Fos (gMFI), JunB (gMFI), FosB (gMFI)

Counts — Fos, JunB, FosB

WT, *Foxo1*-KO, *Foxo1*-AAA

C

Naïve — FOXO1 ChIP-seq, ATAC (WT, *Foxo1*-KO)

Post-infection — FOXO1 ChIP-seq (Day 12), ATAC (Day 7) WT, *Foxo1*-KO

KLRG1^low, KLRG1^high

Fos, *Junb*, *Fosb*, *Jund*

Figure 2

Figure 2 Delpoux et al.

A

B

C
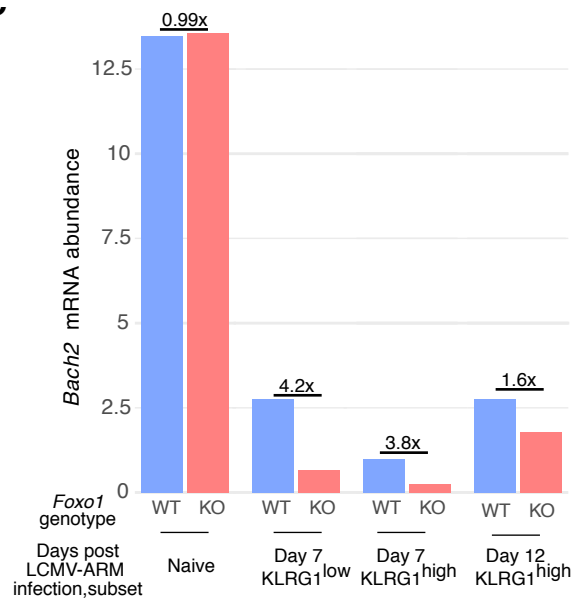
D
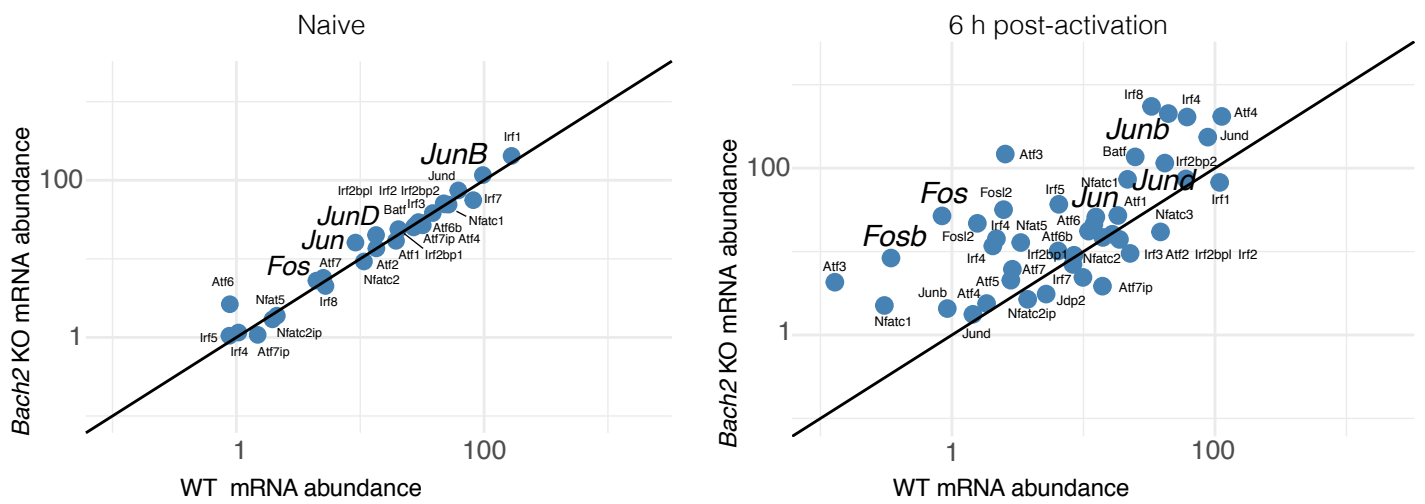
Figure 3

Figure 3 Delpoux et al.
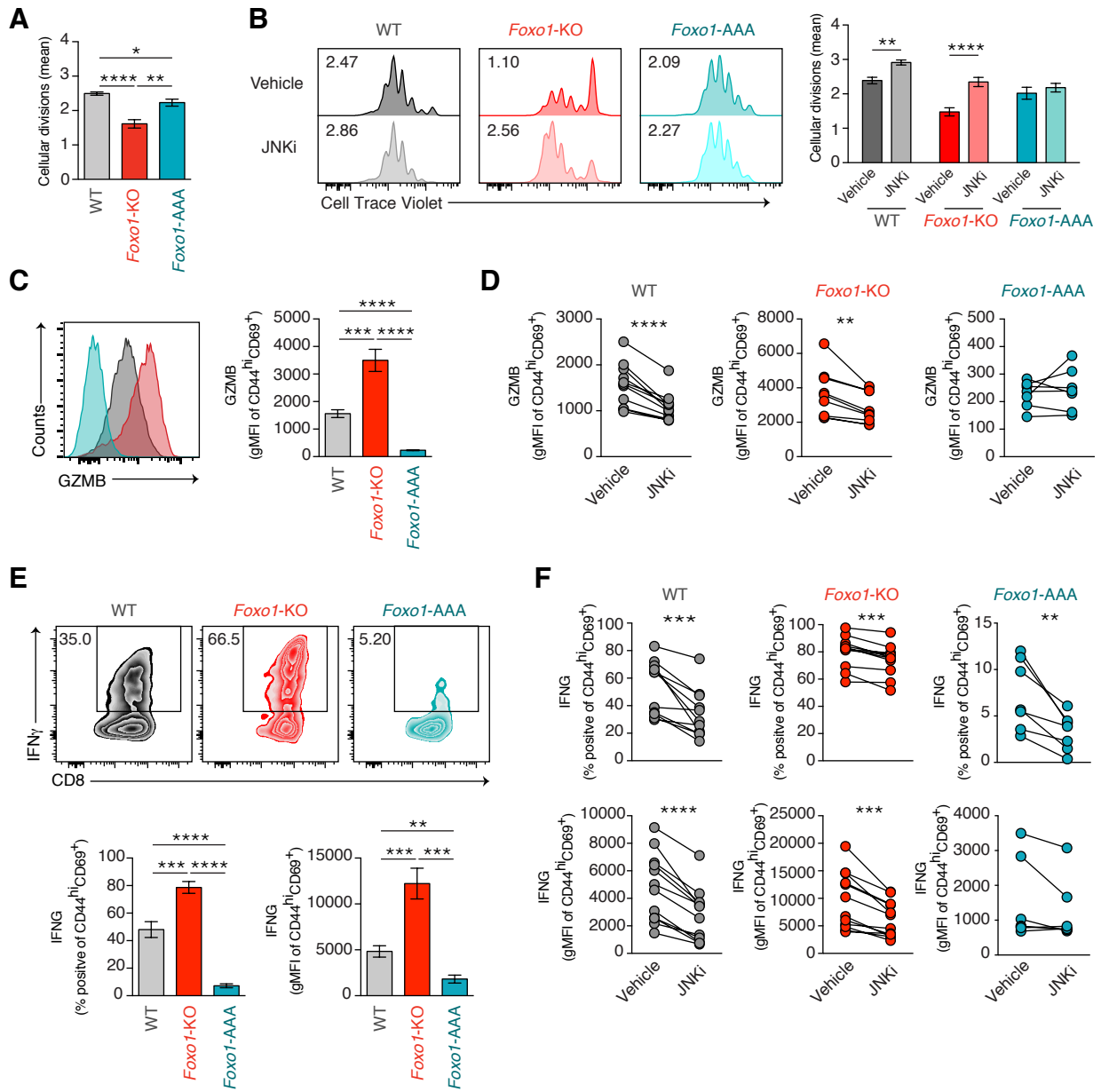
Figure 4

Figure 4 Delpoux et al.
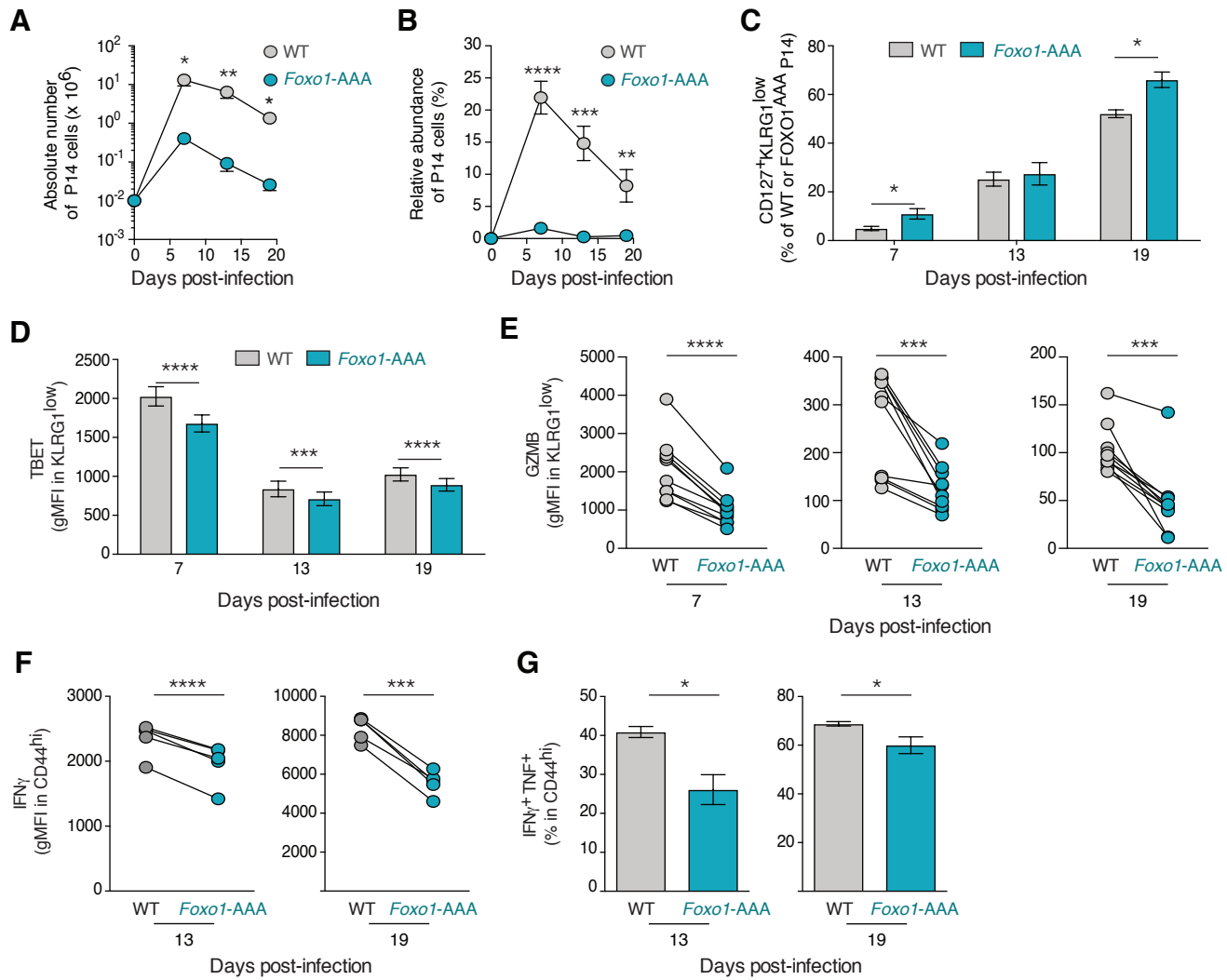
Figure 5

Figure 5 Delpoux et al.
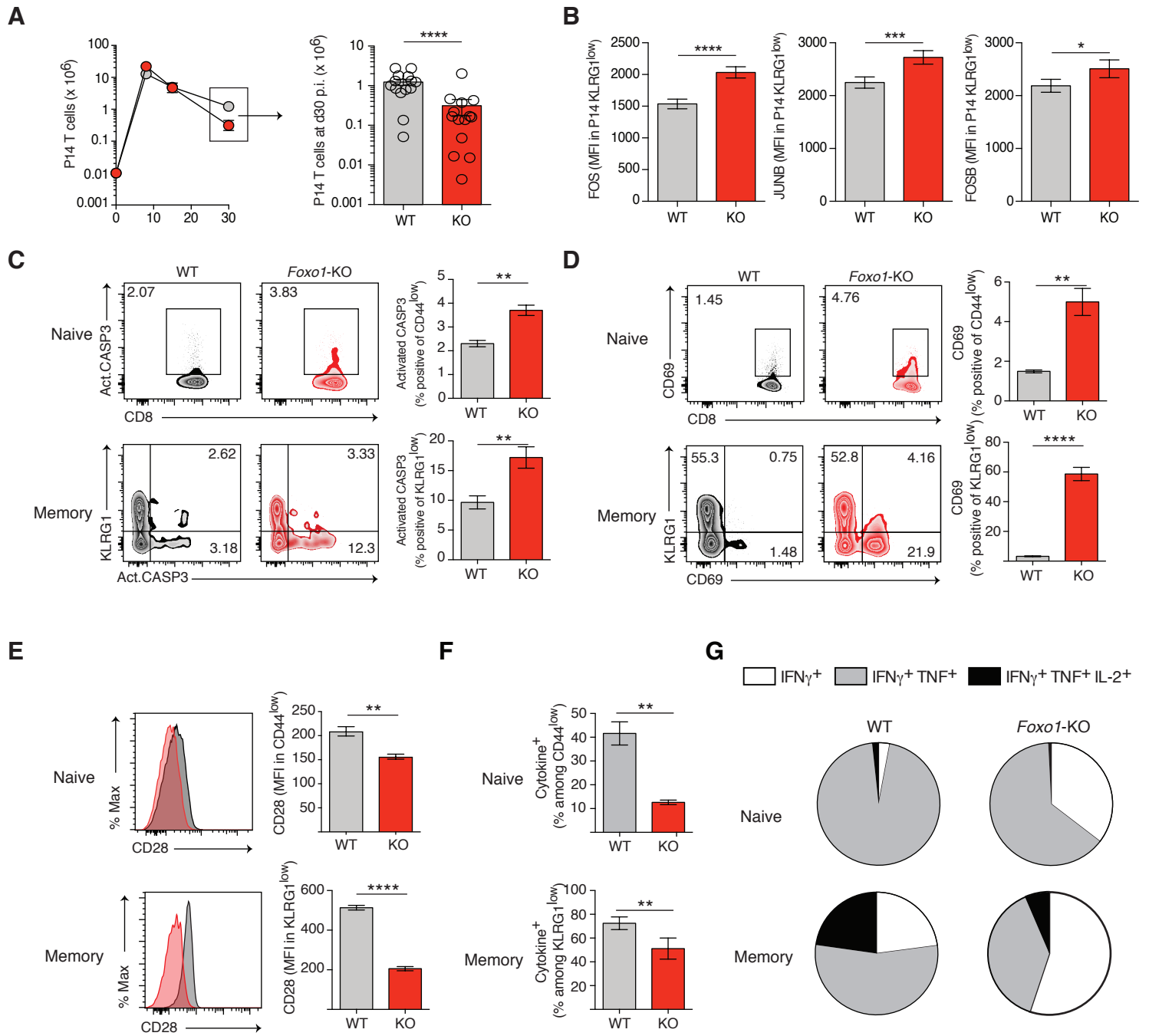
Figure 6

Figure 6 Delpoux et al.
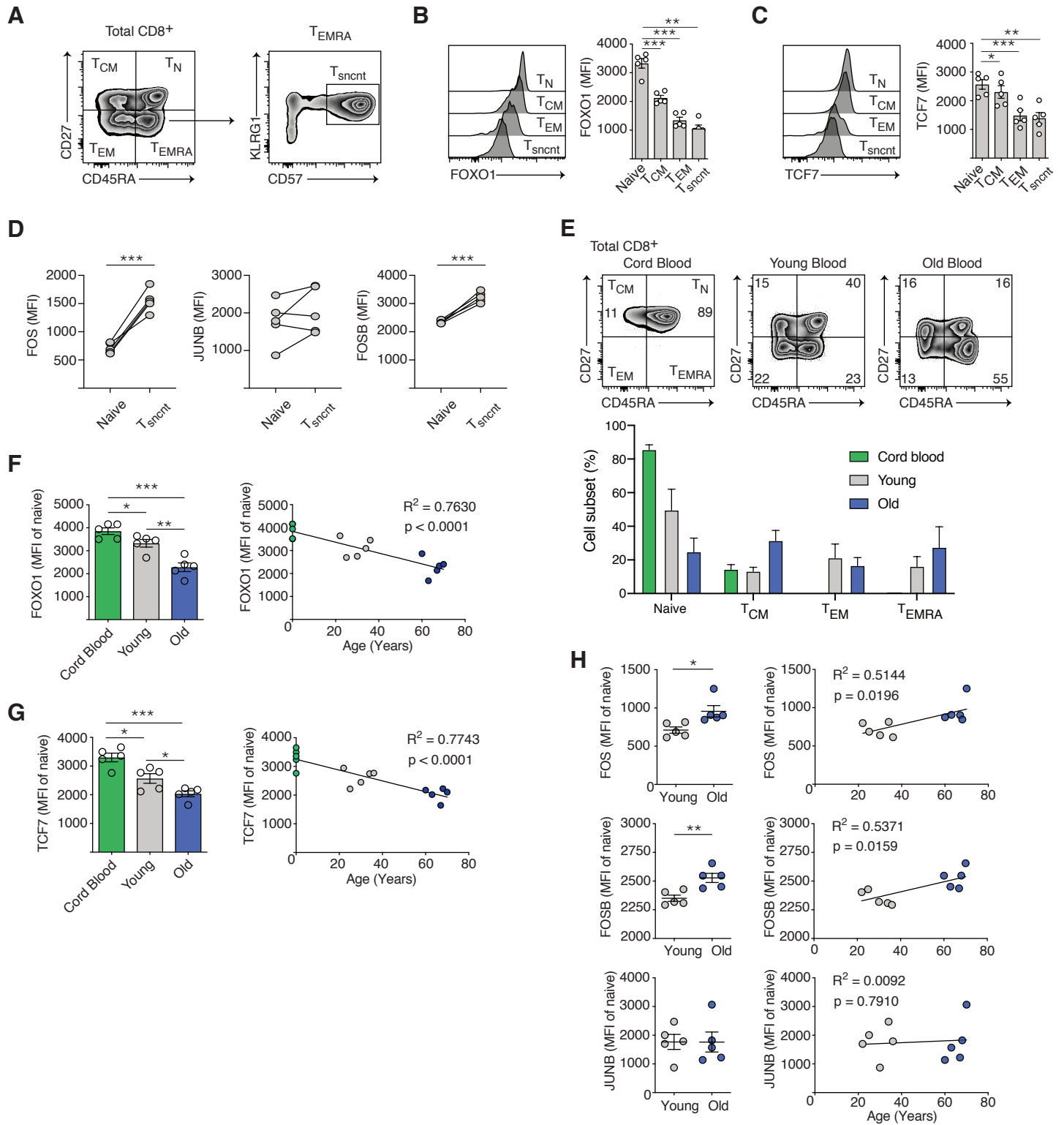
Figure S1 Delpoux et al.

A

B

C
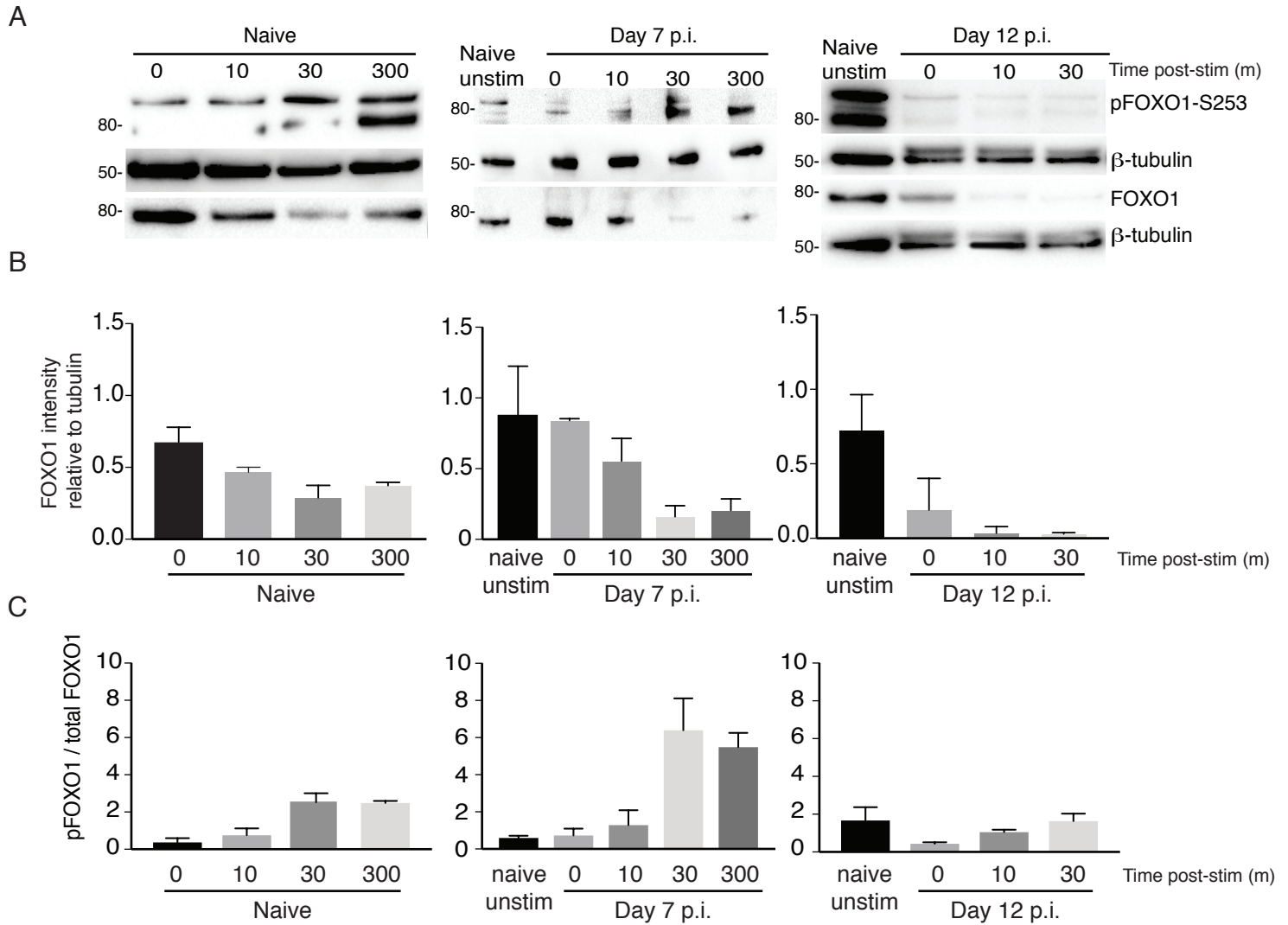
Figure S1: **Restimulation kinetics of total FOXO1 and phospho-FOXO1-S253 from naive and post-infection antigen-specific CD8+ T cells, related to Figures 1 and 2.** Naive or adoptively transferred WT P14 CD45.1 CD8+ naïve T cells into C57BL/6 (CD45.2) host at day-1 and infected with LCMV-ARM on day 0. Related to Figure 1. (**A**) Representative immunoblots probed for phospho-FOXO1-S253, stripped and re-probed for total FOXO1, in lysates of naïve CD8+ T cells or in CD45.1+ T cells. T cells were isolated from LCMV-ARM infected mice on days 7 and 12, stimulated *in vitro* for the indicated time. For day 12 samples, total FOXO1 was probed on separate membrane. Numbers to the left indicate molecular weight markers (kDa). (**B**) Quantitation of total FOXO1 relative to tubulin and (**C**) phospho-FOXO1-S253 relative to total FOXO1. The data are cumulative from 2 (naïve and day 12) or 3 (day 7) mice per group.
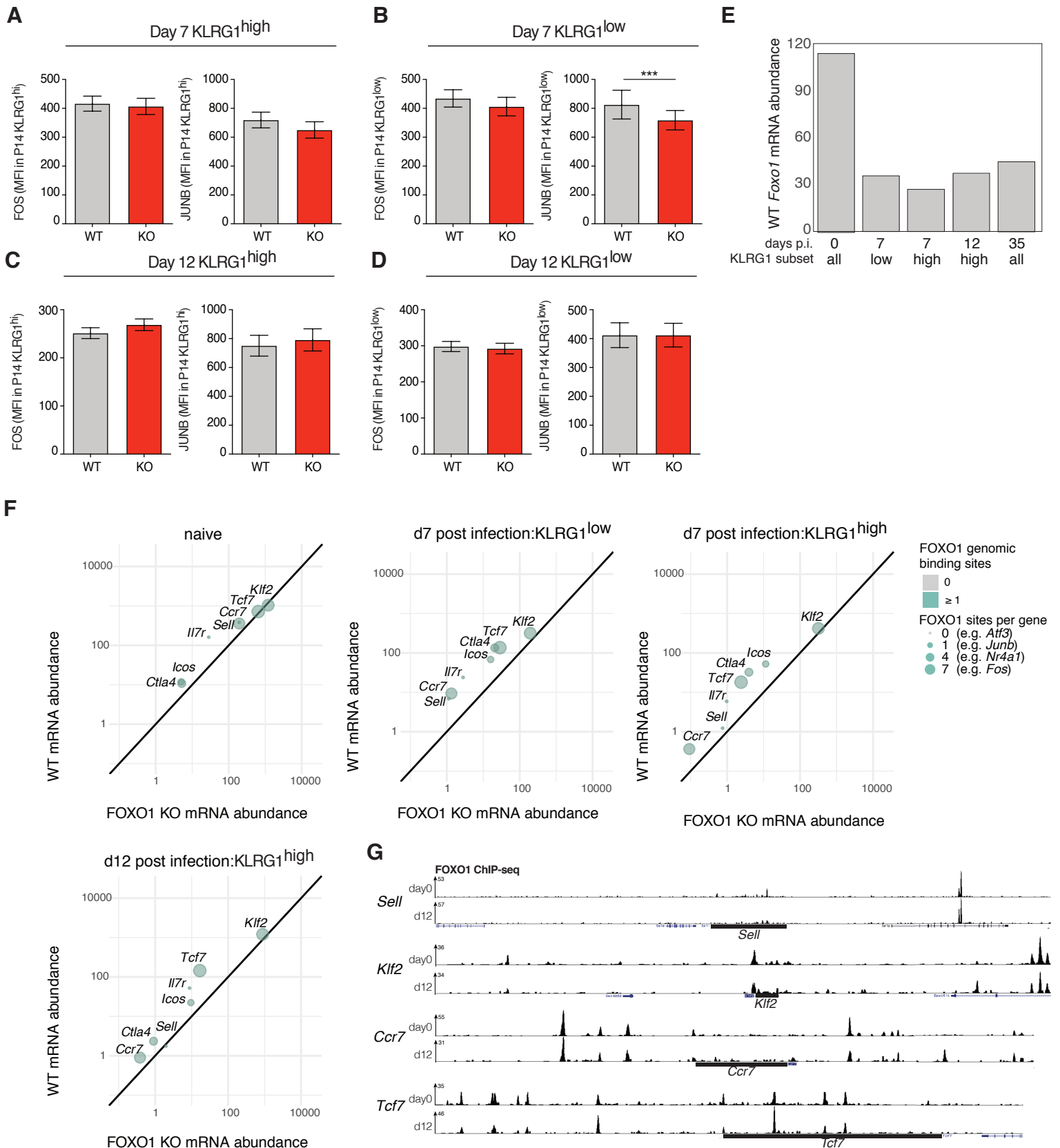
Figure S2: **FOXO1 regulates key target genes despite limited regulation of AP-1 factor protein abundance at day 7 or day 12 post-activation, related to Figure 2**. (A-D) A mixed adoptive transfer of P14 WT and *Foxo1*-KO (*Foxo1*-dLckCre) T cells into WT hosts at day -1 and infection with LCMV-ARM on day 0. (A,B) FOS and JUNB immunostaining was determined at day 7 and at (C, D) day 12 p.i in KLRG1hi and KLRG1low T cells. (E, F) RNA-seq quantitation of (E) *Foxo1* RNA abundance in indicated P14 T cell populations before or after infection and of (F) indicated trafficking molecules/known FOXO1 targets; same dataset/methods as Figs.1 and 2. (G) FOXO1 ChIP-seq of genomic loci of indicated genes, same dataset/methods as Figs 1 and 2. (A-D) Data are from one representative experiment from two experiments with n=4 mice per group and per time point. * $P < 0.05$; ** $P < 0.01$; *** $P < 0.001$; **** $P < 0.0001$; paired Student's t test was used and error bars represent mean ± SEM.
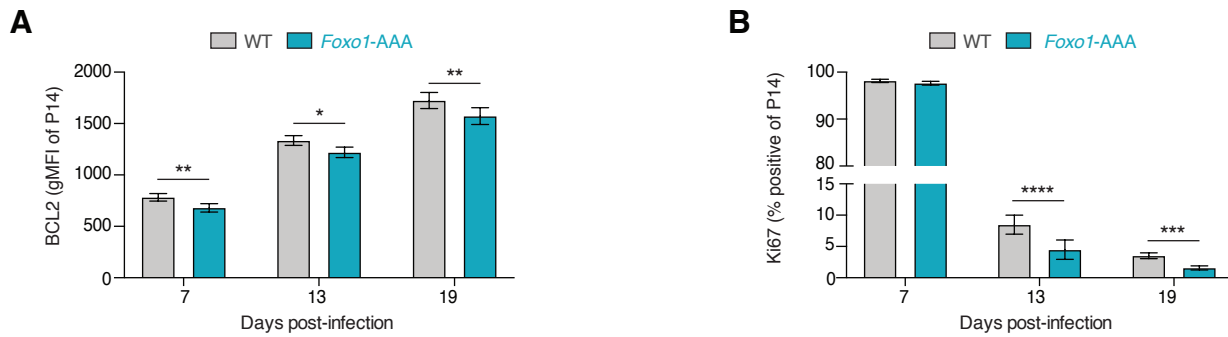
Figure S3: **Effect of nuclear expression of FOXO1 on BCL2 and Ki67, related to Figure 4.** A mixed adoptive transfer of WT P14 and Foxo1-AAA P14 T cells into WT hosts at day -1, infected with LCMV-ARM on day 0. Graphs depict BCL-2 MFI or percentage of Ki67^{+} cells at days 7, 13 and 19 post-infection. Data are cumulative from 2 experiments with n= 4 to 5 mice per group and per time point. * $P < 0.05$; ** $P < 0.01$; *** $P < 0.001$; **** $P < 0.0001$; paired Student's t test was used and error bars represent mean ± SEM.
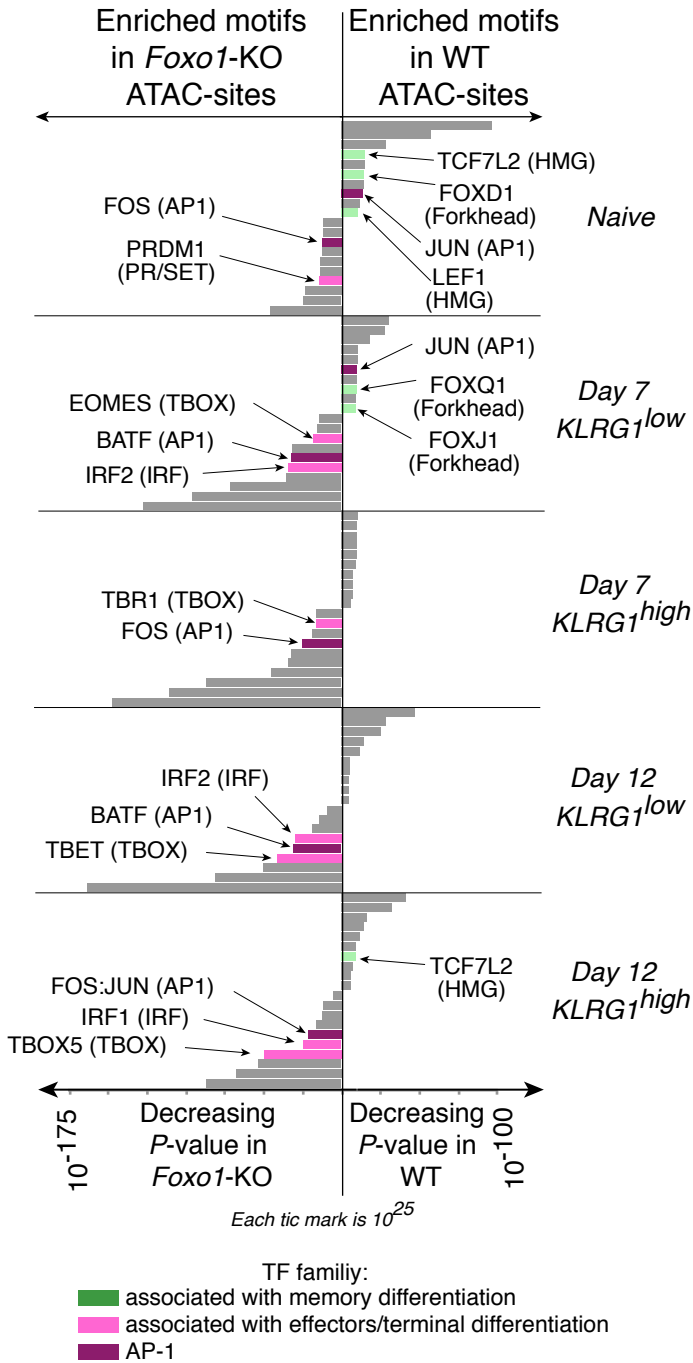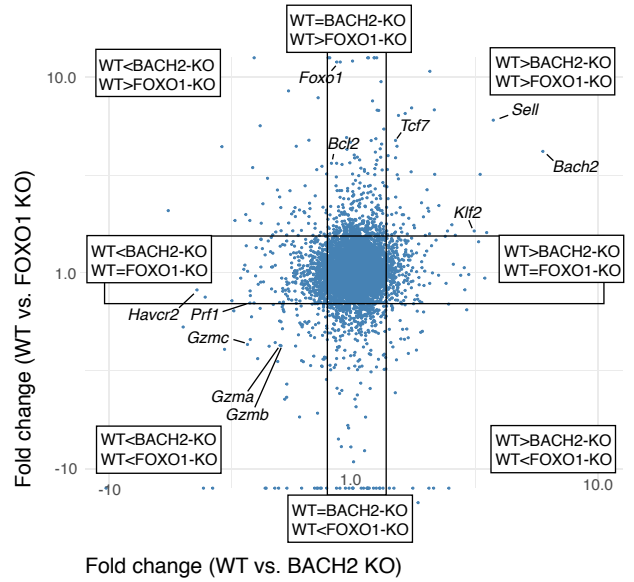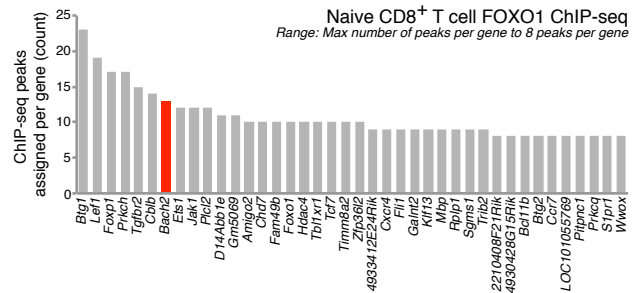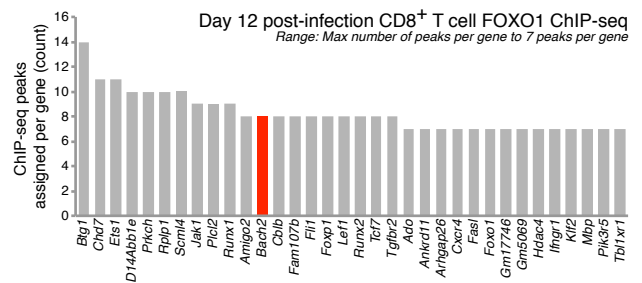
Figure S4: ***Foxo1*-KO cells exhibit increased AP-1 and effector-associated TF binding site abundance in sites of differential chromatin accessibility, related to Figures 1 and 2. (A)** Sites of differential DNA-accessibility (determined by ATAC-seq) between WT P14 and FOXO1 KO P14 cells were determined in pairwise fashion in naive cells, or at the indicated days post-infection with LCMV-ARM, and then transcription factor binding motifs were identified within these regions of differential genomic accessibility. The first ten motifs detected, ordered by increasing P-value were displayed (in some cases, less than ten were detected; P-value derived from the likelihood of finding the motif at the observed frequency in background DNA). **(B)** Fold-change of BACH2 KO vs WT (data downloaded from GSE77857) plotted against FOXO1 vs WT (same methods and dataset as in Figs. 1 and 2). **(C)** Number of FOXO1 genomic binding sites assigned per gene from ChIP-seq -> HOMER analysis of naive and **(D)** day 12 post-activation FOXO1 (ChIP-seq from Fig1 and 2; see methods). For A, HOMER was used for ATAC seq peak calling and transcription factor motif finding; see methods)
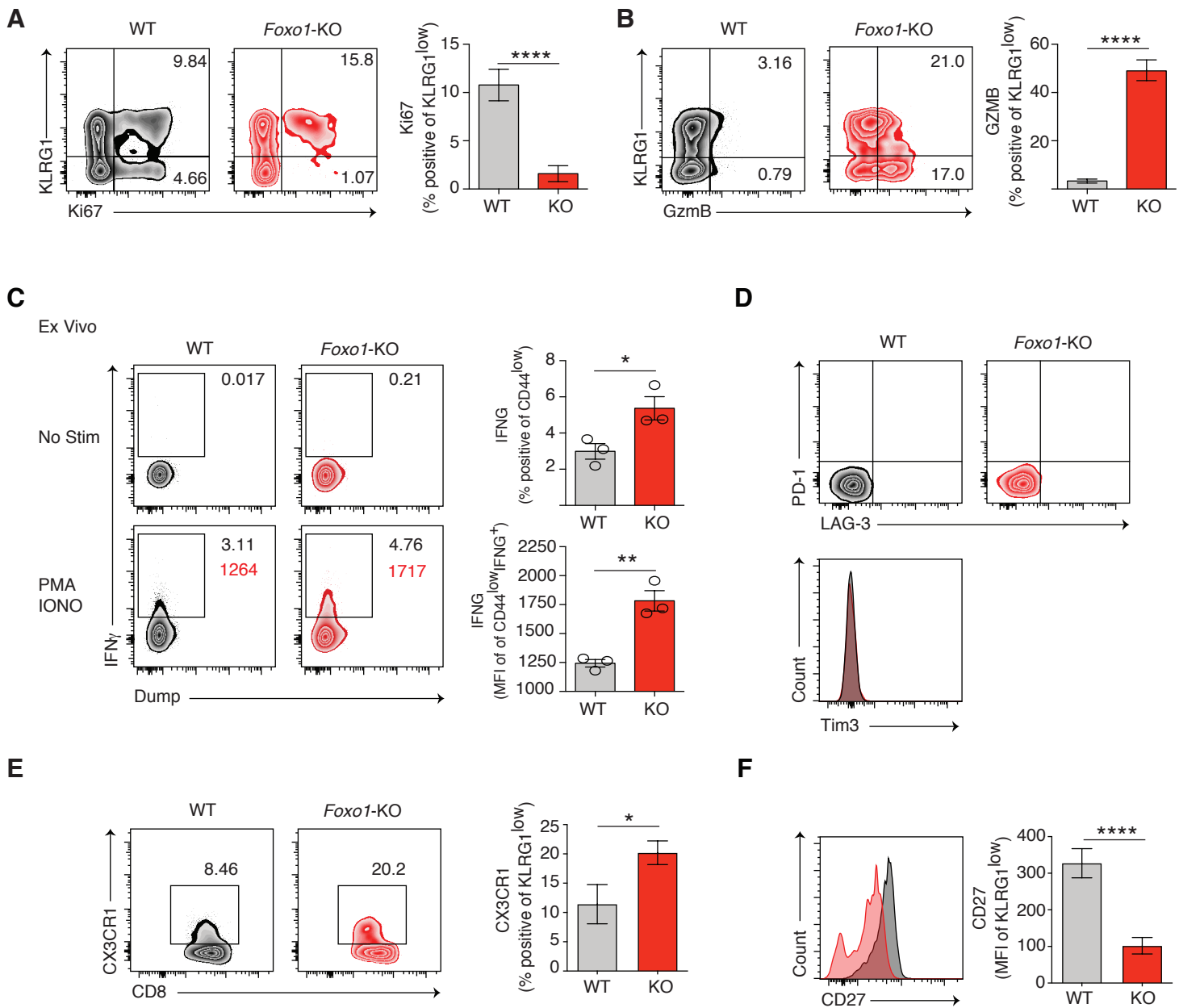
Figure S5 Delpoux et al.

Figure S5: **Naive and memory *Foxo1*-KO CD8 T cell exhibit a senescent phenotype, related to Figure 5. (A-B)** A 1:1 mixed adoptive transfer of WT P14 and FOXO1-KO P14 T cells into WT hosts at day -1, infection with LCMV-ARM on day 0. (**A**) Expression of KLRG1 and Ki-67 by WT and FOXO1 KO P14 at day 30 p.i. (**B**) Expression of KLRG1 and GZMB by WT and *Foxo1*-KO P14 cells at day 30 p.i. (**C**) Expression of IFNγ and dump channel among WT and *Foxo1*-KO naive (CD44low) cells without stimulation (upper panel) or after 4 hours of PMA + IONO stimulation (lower panel). Numbers indicate the percentage (black) or MFI (red) of IFNγ+ T cells. (**D**) Expression of PD-1, LAG-3, and TIM3 on WT and Foxo1 KO T cells day 30 p.i. (**E**) Expression of CX3CR1 on WT and *Foxo1*-KO KLRG1low P14 cells day 30 p.i. (**F**) Expression of CD27 on WT and FOXO1 KO KLRG1low P14 cells day 30 p.i. (A and B) Data are cumulative from 3 experiments with minimum n=3 mice per group and per time point. **(C-F)** One representative experiment is shown from 2 experiments with 3 mice per group *P < 0.05; **P < 0.01; ***P < 0.001; ****P < 0.0001; unpaired Student's t test was used (C), paired Student's t test was used (A-B) and error bars represent mean ± SEM.
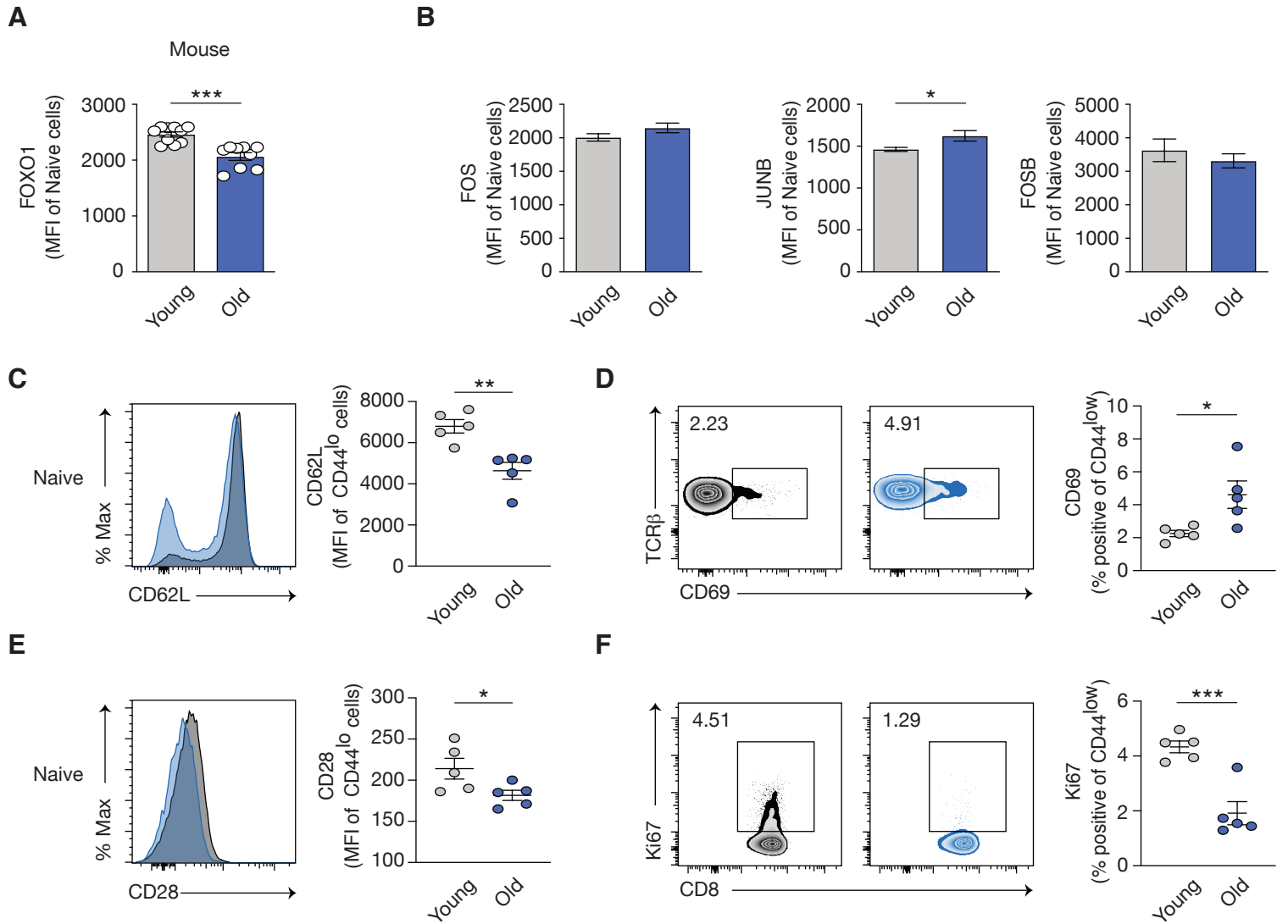
Figure S6: **Age-dependent, inverse correlation of FOXO1 and AP-1 subunit abundance in T cells from young and old mice, related to Figure 6.** (**A**) Bar plots depicting FOXO1 expression in naive CD8$^+$TCRβ^+CD44^{low} cells from young (3 months) and old (>18 months) mice. (**B**) FOS, JUNB and FOSB abundance in naive CD8$^+$ T cells in young and old mice. (**C**) Histogram (left) shows CD62L abundance among naive CD8$^+$ T cells in young and old mice. Scatter plot (right) depicts CD62L MFI. (**D**) Expression of TCRβ and CD69 on naive CD8$^+$ T cells in young and old mice. Scatter plot (right) indicates the percentage of CD69$^+$ among naive CD8$^+$ T cells in young and old mice. (**E**) CD28 abundance among naive CD8$^+$ T cells in young and old mice. (**F**) Expression of Ki67 and CD8 on naive CD8$^+$ T cells from young and old mice. (A) Data are cumulative from 2 experiments with 5 mice per group and per experiment. (B-F) Data are representative of one experiment from 2 experiments with 5 mice per group. (*P < 0.05; **P < 0.01; ***P < 0.001; ****P < 0.0001; unpaired Student's t test were used and error bars represent mean ± SEM.